

Resistivity survey in Alid geothermal area, Eritrea

Hjálmar Eysteinnsson
Andemariam Teklesenbet
Guðni Karl Rosenkjær
Ragna Karlsdóttir

Prepared for ICEIDA (ÞSSÍ)

Report no. ÍSOR-2009/016	Date February 2009	Distribution <input checked="" type="checkbox"/> Open <input type="checkbox"/> Closed
Report name / Main and subheadings Resistivity survey in Alid geothermal area, Eritrea	Number of copies 10	Number of pages 42 + Appendices
Authors Hjálmar Eysteinnsson, Andemariam Teklesenbet, Guðni Karl Rosenkjær and Ragna Karlsdóttir	Project manager Hjálmar Eysteinnsson	
Classification of report	Project no. 590112	
Prepared for ICEIDA (Þróunarsamvinnustofnun Íslands)		
Cooperators		
<p>Abstract</p> <p>A geophysical survey of the Mt. Alid geothermal area in Eritrea was performed in late 2008. The aim of the survey was to delineate if possible the geothermal reservoir by the use of TEM and MT soundings. The original plan was to cover the area of Mt. Alid and its nearest vicinity. The terrain however was very difficult for vehicles and bikes used for transportation of the equipment and inaccessible at times. Within given timeframe the area to the west and southwest of the mountain was covered as well as the top of Mt. Alid.</p> <p>The resistivity survey only reveals a part of the geothermal reservoir, due to lack of soundings. A SW-NE lineament is detected at a depth interval 500 metres to 2 km, interpreted as a transform fault intersecting the geothermal reservoir and most likely controls the main upflow into the reservoir.</p> <p>At the surface at the southwest flanks of Mt. Alid, an area with exceptional vegetation in comparison to the barren dry volcanic landscape around, indicates moisture and water in the ground that could be explained by steam upflow from the geothermal reservoir.</p>		
Key words Eritrea, Mt. Alid, resistivity survey, geothermal reservoir, fault, upflow zone	ISBN-number	
	Project manager's signature	
	Reviewed by KÁ, BS	

Table of contents

1	Introduction.....	7
2	Geological settings for Mt. Alid geothermal field.....	8
3	Field survey	9
4	Data acquisition.....	12
4.1	The survey area	13
4.2	TEM data	13
4.3	MT data	14
4.4	Telluric shift in MT soundings	20
5	Result of joined inversion of MT and TEM data	22
5.1	Resistivity maps	22
5.2	Resistivity cross sections	26
6	Conclusions and recommendations.....	37
7	References.....	42
	Appendices	
1.	TEM and MT soundings, coordinates and elevation.....	
2.	TEM data	
3.	MT data Z.....	
4.	MT data apparent resistivity and phase.....	
5.	1-D interpretation models for joint TEM/MT inversion	
6.	Resistivity maps	

List of figures

Figure 1.	<i>The location of Mt. Alid geothermal field.</i>	7
Figure 2.	<i>The east African rift system</i>	8
Figure 3.	<i>The camp at Buya</i>	9
Figure 4.	<i>Original plan for the MT/TEM soundings</i>	10
Figure 5.	<i>The sixwheel-bikes used for transportation of the equipment in the field</i>	10
Figure 6.	<i>Location of TEM and MT soundings</i>	11
Figure 7.	<i>Preparing for the tour to Mount Alid</i>	12
Figure 8.	<i>TEM survey on Mount Alid</i>	13
Figure 9.	<i>Performing MT measurements</i>	14
Figure 10.	<i>Impedance elements for MT site 006 with the amplitude on the left and the phase on the right</i>	16
Figure 11.	<i>Rose diagrams of strike directions for all frequencies of all the MT sites</i>	17
Figure 12.	<i>Rose diagrams of strike directions for periods greater than 10 seconds, for all the MT sites</i>	18

Figure 13. <i>Apparent resistivity and phase for two sites</i>	19
Figure 14. <i>An example of a joint inversion result of TEM- and MT data</i>	20
Figure 15. <i>Histogram of shift factors applied to the MT apparent resistivity curves</i>	21
Figure 16. <i>Fixing one of the bikes in a difficult terrain</i>	22
Figure 17. <i>Resistivity map at 100 metres below sea level</i>	23
Figure 18. <i>Resistivity map at 500 metres below sea level</i>	23
Figure 19. <i>Resistivity map at 1000 metres below sea level</i>	24
Figure 20. <i>Resistivity map at 3500 metres below sea level</i>	25
Figure 21. <i>Location of cross sections</i>	26
Figure 22. <i>A resistivity cross section through the area, with NW-SE direction</i>	27
Figure 23. <i>Cross section WE1640</i>	29
Figure 24. <i>Cross section WE1641</i>	29
Figure 25. <i>Cross section WE1642</i>	30
Figure 26. <i>Cross section WE1643</i>	30
Figure 27. <i>Cross section WE1644</i>	31
Figure 28. <i>Cross section WE1645</i>	31
Figure 29. <i>Cross section WE1646</i>	32
Figure 30. <i>Cross section WE1647</i>	32
Figure 31. <i>Cross section SN593</i>	33
Figure 32. <i>Cross section SN594</i>	33
Figure 33. <i>Cross section SN595</i>	34
Figure 34. <i>Cross section SN596</i>	34
Figure 35. <i>Cross section SN597</i>	35
Figure 36. <i>Cross section SN598</i>	35
Figure 37. <i>Cross section SN599</i>	36
Figure 38. <i>Conclusions</i>	37
Figure 39. <i>An oases in the middle of the dry volcanic landscape</i>	38
Figure 40. <i>An aerial photo of Mt. Alid and part of the Danakil depression from Google-earth</i>	40

1 Introduction

In October 2008 the Iceland GeoSurvey (ISOR) signed an agreement with Icelandic Developing Agency (ICEDA), concerning ISORs implementation of a geophysical survey in the Mount-Alid geothermal region in Eritrea (Figure 1). The survey should consist of magneto-telluric (MT) and central loop transient electromagnetic (TEM) soundings at and in the nearest vicinity of Mt Alid. Iceland Geosurvey made a cooperation agreement with the Geological Survey of Eritrea (GSE, under the Eritrean ministry of energy and mines) concerning this survey. The field survey was led by Dr. Hjálmar Eysteinnsson, geophysicist from ISOR, and Andemariam Teklesenbet, geophysicist from GSE. The Geological Survey of Eritrea provided geoscientists to participate in the survey and make necessary preparatory arrangements. The geophysical exploration was planned to last for 30 working days in the field and the amount of 100 soundings of both MT and TEM was expected to be measured.



Figure 1. The location of Mt. Alid geothermal field.

2 Geological settings for Mt. Alid geothermal field

Alid volcanic center, Eritrea, is located along the axis of the Danakil depression, the graben trace of a crustal spreading center that radiates NNW from a plate-tectonic triple junction situated within complexly rifted and faulted basaltic lowland called the Afar triangle (Figure 2). The Danakil depression is a subaerial segment of the spreading system that is opening to form the Red Sea. Crustal spreading along the axis of the Red Sea is transferred to spreading along the Danakil segment in a right stepping en echelon pattern (Barberi and Varet, 1977). The northern Danakil depression lies near or below sea level for the most of its extent. It is surrounded by the Danakil horst to the east and the Eritrean plateau to the west.

The Alid mountain rises up to about 700 metres above the flat plains of the Danakil depression, to a summit of 904m. The mountain is elongated with major axis of 7 km in ENE-WSW direction, perpendicular to the graben, and a minor axis is about 5 km long parallel to the graben. MT. Alid is a structural dome with rocks subdivided from oldest to youngest into: 1) Precambrian basement; 2) Interlayered sedimentary deposits and lava-flows; and 3) Basaltic and rhyolitic lava-flows (Clynne et al., 2005).

Geological and geochemical studies imply that a high temperature geothermal system underlies the Alid volcanic center. Fumaroles and boiling pools on the northern part of Mt. Alid suggest that an active hydrothermal system underlies that part of the mountain. Geothermometers indicate temperatures exceeding 250 °C in the reservoir (Lowenstern et al., 1999; Clynne et al., 2005).

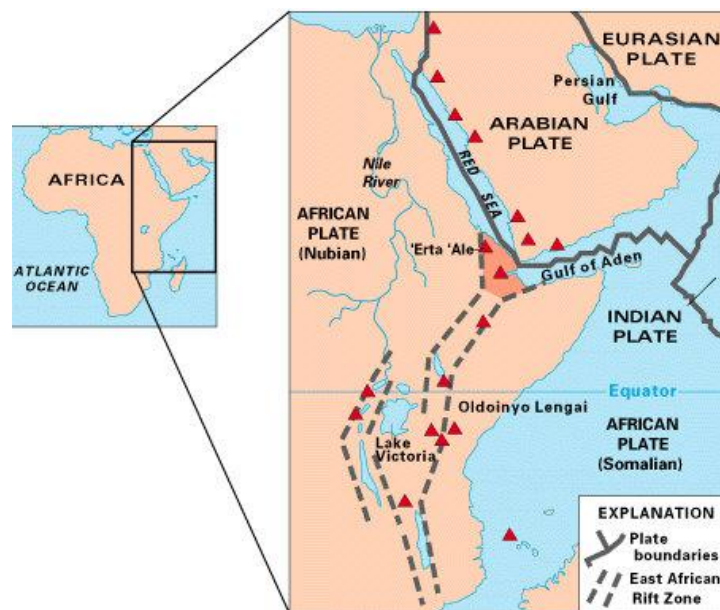


Figure 2. The east African rift system, showing some of the historically active volcanoes (red triangles) and the Afar Triangle (shaded, center) — a triple junction where three plates are pulling away from one another: the Arabian Plate, and the two parts of the African Plate (the Nubian and the Somalian) splitting along the East African Rift Zone..

3 Field survey

Prior to the fieldwork period, Mr. Porleifur Finnson went to Djibouti on behalf of ISOR to take care of shipping of four six-wheel bikes and other equipment from Djibouti to Eritrea. The bikes had been used in Djibouti in a similar survey by ISOR. Prior attempts to get the bikes shipped to Eritrea had not been successful. He also made a trip to Eritrea for the preparations for the survey, i.e. finished the contract with the GSE, opened a bank account, visited the survey area and the proposed camping area, arranged custom clearance of the bikes etc. Due to financial crises in Iceland at this time no money could be transferred to Eritrea while Porleifur was there and therefore he could not arrange the setup of the base camp.

Two geophysicist from Iceland GeoSurvey arrived to Asmara, the capital of Eritrea, in the evening of November 10th. It took more than a week to prepare for the fieldwork. Custom clearance of all the equipment took a long time, and permission for using a satellite phone in the field was extremely difficult to get. Getting all necessary appliances for the field (refrigerator, freezer, furniture etc.) and food was also time consuming. On the 19th of November the survey crew left Asmara. All the gear had been loaded on one truck and the two pickups to be used in the field. Another truck was loaded in Massawa with the equipment and the four 6weel bikes that came from Djibouti. The group arrived in the Alid field, to the village of Buya well after midnight (Figure 3).



Figure 3. *The camp at Buya (photo: Hjálmar Eysteinnsson).*

The next day the camp was set up, the two trucks were unloaded, tents where set up, kitchen made clear, bikes where made ready etc. The day after, on the 21st of November, the first TEM soundings where done, and the MT equipment calibrated and an MT base station installed (for remote reference). The survey continued until 14th of December, when the last soundings where done and the equipments where collected and the MT instruments calibrated.

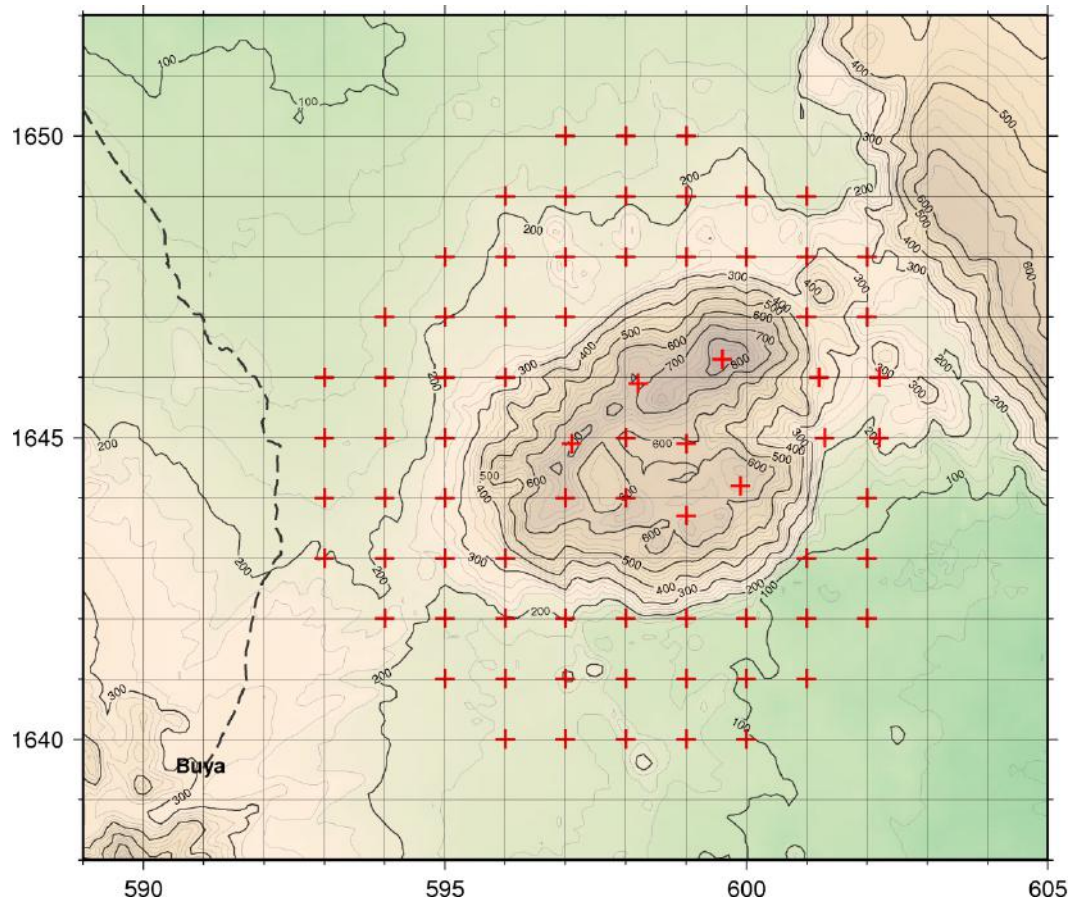


Figure 4. Original plan for the MT/TEM soundings. (Scale is UTM coordinates, in km, zone37).



Figure 5. The sixwheel-bikes used for transportation of the equipment in the field (photo: Hjálmar Eysteinnsson).

Four units of MT equipments were used in the survey, where one served as a base or reference station measuring a continuous MT signal and used for reference signal to give better data quality, a method named remote reference. One set of TEM equipment was in use.

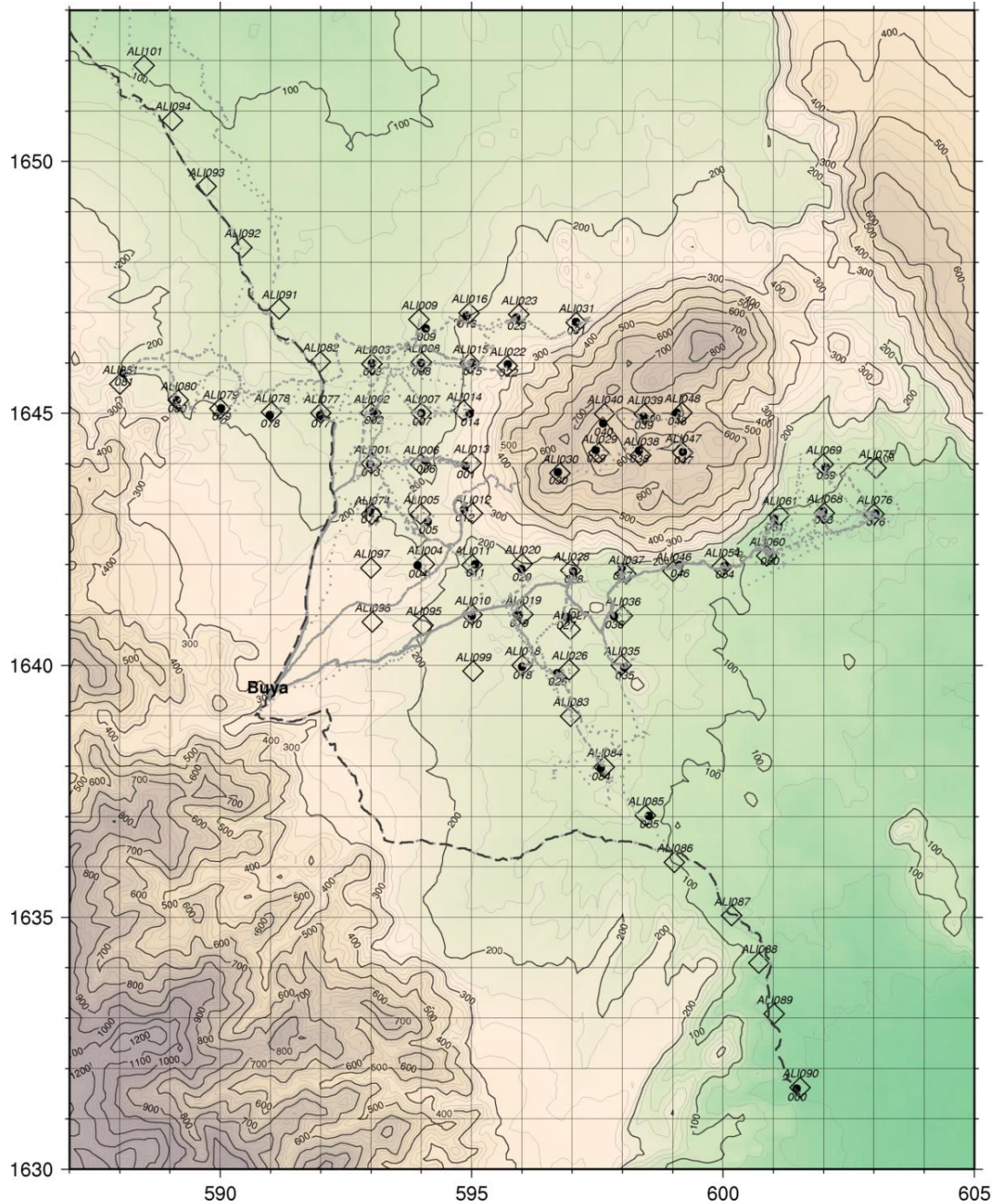


Figure 6. Location of TEM (open diamonds, with the name above) and MT soundings (filled points with the name below). Roads and tracks used are shown as black dashed lines and gray lines respectively. Coordinates are in UTM, km units.

On the 15th of December the field crew left Buya. One truck carried the bikes to Massawa, and another carried the rest of the field gear to Asmara. After some delay in Massawa the bikes were finally put into a container to be shipped back to Djibouti. The convoy arrived to Asmara late in the evening. On the 16th we finished all the payments that needed to be done and closed the bank account. The ISOR personnel left for Iceland on the 17th of December.

As said before, the field survey was led by Dr. Hjalmar Eysteinnsson (geophysicist) from Iceland GeoSurvey (ISOR), and Andemariam Teklesenbet (geophysicist) from EGS. Other participants were Guðni Karl Rosenkjær (geophysicist) from ISOR, Yonas Estianos (EGS geologist) Mussie Beraki (EGS geologist), Debesay Habte (EGS, field assistant), Rigat (cook), Azieb Hagos (cook), Birhane Sultan (driver) and Salihadin (driver). Many local assistants also took part in the project.

4 Data acquisition

During the data acquisition two groups worked in the field, one for each method of measurements. The project leader from Iceland GeoSurvey performed data quality check and a preliminary interpretation of most of the data at base camp as data was collected. During the field work period of 24 days, a total of 52 MT soundings were measured (some of which were repeated due to bad data quality) and 67 TEM soundings (figure 6). This makes 2.2 MT and 2.8 TEM soundings a day on the average. Some days, or part of days, were not productive due to instrument failure. The locations of the soundings are listed in Table 1 in Appendix 1.



Figure 7. *Preparing for the tour to Mount Alid (photo: Hjalmar Eysteinnsson).*

4.1 The survey area

The original plan consisted of 73 MT and TEM soundings shown on Figure 4. As shown, the plan was to carry out the survey on the top of mountain Alid and the area, 2–3 km away from the mountain. This was quite an optimistic plan, considering the time available and the difficult terrain. Some of the area is covered with inaccessible lavaflows. Some time was spent on finding trails into or around the lavafields but without luck. The bikes came to a good use in the field. It was however only possible to do the TEM measurements on the top of Mount Alid by carrying the equipment on the back of camels (Figure 7).



Figure 8. TEM survey on Mount Alid. Note the steam vent in the back (photo: Andemariam Teklesenbet).

4.2 TEM data

In the TEM soundings electrical current is transmitted into a big loop of wire (300x300 m) laid on the ground. This current produces a magnetic field. The current is abruptly turned off and the decaying magnetic field causes induction currents in the ground. The strength of the induced currents is dependent on the resistivity structure below the survey site. The ground response is measured by a small coil in the center of the big transmitting loop. The time decaying signal is measured from 88 μ s to 70 ms from the time of turning of the current.

The TEM instruments used is from Geonics Ltd. in Canada. The TEM soundings can survey the ground resistivity down to about $\frac{1}{2}$ –1 km, depending on the resistivity. For low subsurface resistivity the depth of penetration can be as low as a few hundred meters, but in higher resistivity surroundings it is possible to explore the resistivity down to about 1 km in favorable conditions. For the conditions in the Alid area and the instrument setup, the depth of penetration of the TEM soundings was generally

around 500 meters. One TEM sounding takes a few hours to perform, from the start of setup to the end of the measuring time.

All the TEM data was interpreted in terms of 1-D models (resistivity only varies with depth) using a program developed at ISOR. The TEM data and their interpretation are shown in Appendix 2.



Figure 9. *Performing MT measurements (photo: Hjálmar Eysteinnsson).*

4.3 MT data

In the MT method, the natural fluctuations of the earth's magnetic field are used as signal source. Those fluctuations induce currents in the ground and are measured on the surface with two horizontal and orthogonal electrical dipoles (E_x and E_y) and the magnetic field is measured in three orthogonal directions (H_x , H_y and H_z). It is customary to set the x direction to the magnetic north direction. For simple earth (i.e. homogenous or layered) the electrical field is coherent with its orthogonal source magnetic field (i.e. E_x correlates with H_y , and E_y with H_x) and this relation depends on the earth's resistivity structure.

The MT instruments used here are from Phoenix Ltd. in Canada (MTU type), and can measure the MT signals in the frequency range from 320 Hz up to DC. Four MT units were used in this survey. One 5 component (i.e. E_x , E_y , H_x , H_y and H_z) station was kept running continuously at the same location some 10 km south of the survey area and used for remote reference data processing. This is a standard method to get better quality data from the processing. The other three sites were deployed each day and picked up the next day. This gives about 20 hours of continuous time series, and MT data in the range from 320 Hz (0.003 sec) to about 1000 seconds. The short-period MT data (high frequency) is mainly dependent on the shallow structures due to their short depth of penetration, whereas the long period data are mainly dependent on the

deeper structures. The MT method has the greatest exploration depth of all resistivity methods (some tens or hundreds of kilometers) and is practically the only method for studying deep resistivity structures. In this survey, the exploration depth of the MT soundings was around 10 km, but varied quite much depending on data quality and the resistivity structure.

Three of the MT units are 5 components and one is a two component unit (i.e. measures only E_x and E_y). The two component unit is always set up close to a nearby 5 component site (usually around 1km), and the magnetic field at that site is used for analyzing the result at the two component site. This is of course only valid if the magnetic field is homogeneous locally, an assumption which is usually valid for short distances. In the middle of the field work period, one of the 5 component MT unit broke down in such a way that it was not possible to measure the magnetic field, and therefore it was used thereafter as a two component unit. This made more restriction on where the three MT units were located.

The quality of the MT data was not always satisfactory and therefore many sites had to be re-measured. The main reason for this was low signal strength. The source for the MT signal are mainly thunderstorms in the equatorial belt of the earth (high frequency) and solar storms interacting with the earth's magnetic field (low frequency). During the survey time the solar activity was at the minimum level in it's 11 years activity period, so low signals where expected. In the beginning the electrode dipole length was kept 50 meters but was increased using all the extra wire at hand up to 125 meters. That usually gave better data quality. The electrodes where also refilled with led-chlorite mixture.

Table 2 in Appendix 1, lists the MT soundings, the date of performance, the serial number of the MT unit used and the serial number of the MT unit used for magnetic field in case of a two component site. The electrical dipole length is also shown. For some sites a sounding was done more than once (up to 4 times), these are the instances when data quality was too poor and the soundings had to be repeated.

The measured MT time series are Fourier transformed into the frequency domain and the "best" solution is found that describes the relation between the electrical and magnetic fields through the following equation:

$$\begin{bmatrix} E_x \\ E_y \end{bmatrix} = \begin{bmatrix} Z_{xx} & Z_{xy} \\ Z_{yx} & Z_{yy} \end{bmatrix} \begin{bmatrix} H_x \\ H_y \end{bmatrix}$$

or in matrix notation:

$$\vec{E} = \mathbf{Z}\vec{H}$$

where \vec{E} and \vec{H} are electrical and magnetic vectors (in the frequency domain) and \mathbf{Z} is the complex impedance tensor which contains the information on the subsurface resistivity structure. Programs from Phoenix Ltd. SSMT2000, were used to process the time-series signal using a robust processing method technique. The result was edited in

a MTEDITOR program by Phoenix, and the output was run through a program called edi2edi made by ISOR, which calculates various MT parameters and produces the results in the standard EDI file format. The processed MT data in terms of magnitude and phases of impedance elements are given in Appendix 3.

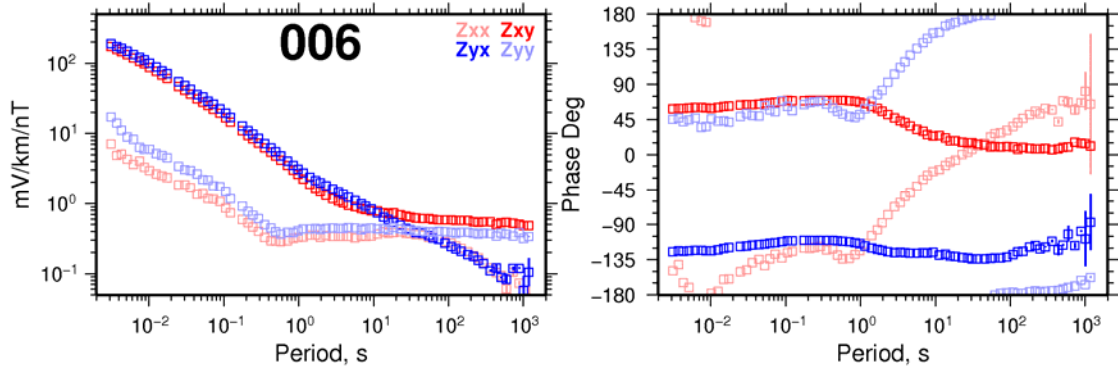


Figure 10. Impedance elements for MT site 006 with the amplitude on the left and the phase on the right. The diagonal elements of the impedance are shown by light red and blue.

The values of the impedance elements are dependent on the resistivity structures below and around the site. For a homogeneous and 1-D earth (resistivity varies only with depth) $Z_{xy} = -Z_{yx}$ and $Z_{xx} = Z_{yy} = 0$. For a 2-D earth, i.e. resistivity varies with depth and in one horizontal direction, it is possible to rotate the coordinate system such that $Z_{xx} = Z_{yy} = 0$, but $Z_{xy} \neq Z_{yx}$. For a 3-D earth all the impedance elements are different. An example of the impedance results for one of the MT sites is shown in Figure 10. As seen there the diagonal elements of the impedance tensor (Z_{xx} and Z_{yy}) are not zero, but they are more than an order of magnitude lower than the off diagonal elements up to about 1 second, and the main impedance elements (Z_{xy} and Z_{yx}) are about the same indicating 1-D resistivity structure for the shallow part. At greater depths, i.e. for periods greater than 10 seconds, all the impedance elements are in the same order of magnitude showing a high degree of three-dimensionality in the resistivity structures below this site.

From the impedances the apparent resistivity and phase is calculated according to

$$\rho_{xy} = 0.2T |Z_{xy}|^2 \cdot; \theta_{xy} = \arg(Z_{xy})$$

$$\rho_{yx} = 0.2T |Z_{yx}|^2 \cdot; \theta_{yx} = \arg(Z_{yx}).$$

Graphs of the apparent resistivity and phases for all the MT soundings are given in Appendix 4. As mentioned earlier the MT impedance is dependent on the orientation of the horizontal electrical and magnetic fields. The rotation that minimizes the diagonal elements in the impedance tensor is called the electrical strike direction, and is also plotted for each site in Appendix 4. The MT parameters in a rotated coordinate system (one fixed rotation angle for all frequencies) are also shown along with the

result of the tipper for those sites where vertical magnetic field was measured (the relation between the vertical- and the horizontal magnetic fields). A rose-diagram rotation plot for the strike direction is shown in Figures 11 for all frequencies and on Figure 12 only for periods greater 10 seconds (the data representing the deeper parts). The figures clearly demonstrate that the main geo-electrical strike is parallel to the rift direction. The rift strike is better represented by the long periods compared to the short periods which are more dependent on the local resistivity close to each site.

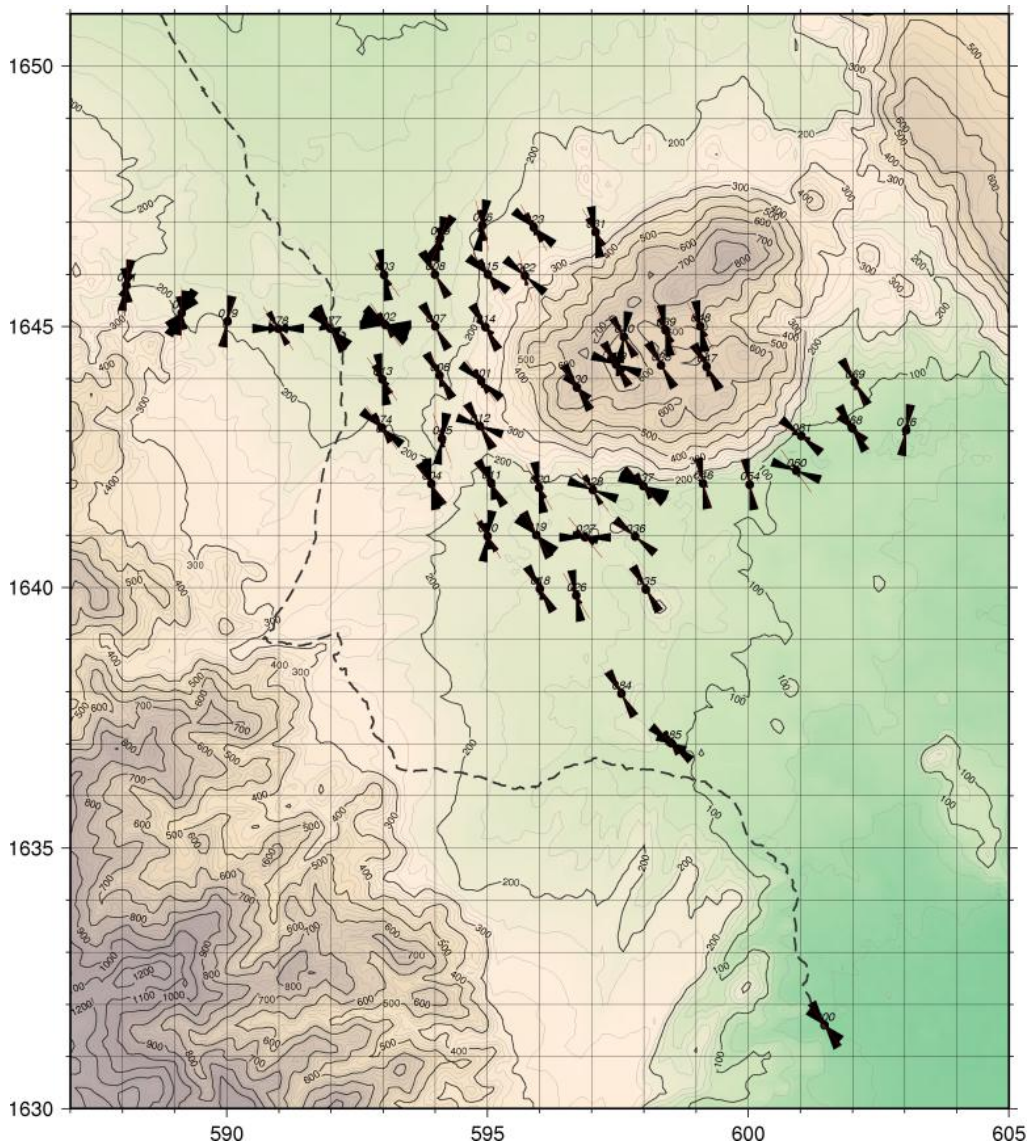


Figure 11. Rose diagrams of strike directions for all frequencies of all the MT sites. The preferred rotation for each site is shown by a red line through each site location.

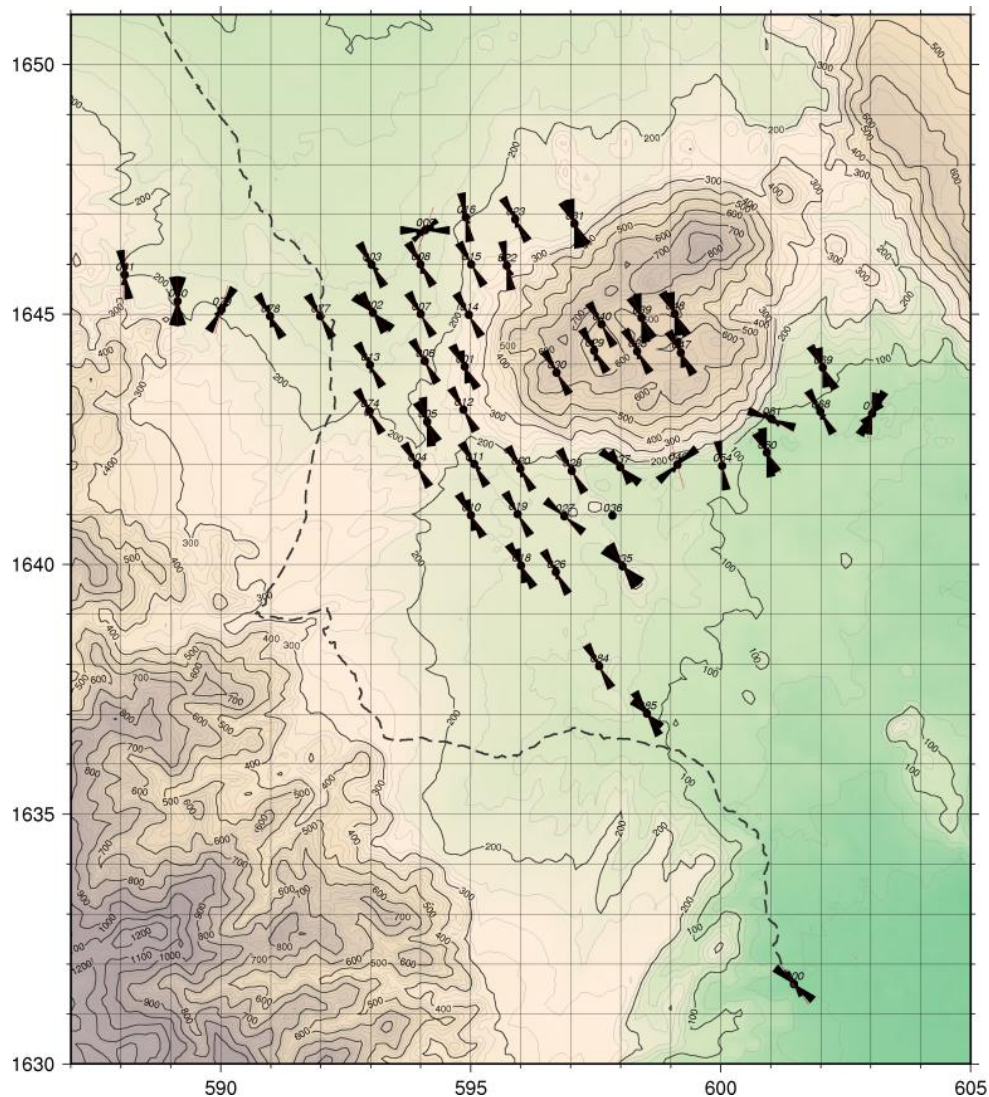


Figure 12. Rose diagrams of strike directions for periods greater than 10 seconds, for all the MT sites. The preferred rotation for each site is shown by a red line through each site.

It is clear from the MT data that the resistivity structures of the Alid area are highly three dimensional. A measure of the three-dimensionality is the so called skew parameter which is the ratio between the magnitude of the sum of the diagonal elements and the magnitude of the difference of the off diagonal elements. This parameter is plotted in Appendix 4 for all the soundings. This parameter is usually less than 0.1 for periods less than 1 second , but increases dramatically for periods greater than 1–10 seconds, to values even greater than 1. Thus it is clear that for a full understanding of the MT parameters a 3-D interpretation of the data is called for. This is however out of the scope of this work since 3-D modeling is very time consuming. A 1-D modeling (horizontal layered earth) of the MT data is quite straightforward and is the only interpretation of the data used in this report. The question is which parameters should be inverted for? In a 3-D data inversion all the impedance elements

are inverted for, where as in a 2-D inversion both the xy and yx pairs are inverted for. But in a 1-D inversion one could invert for either xy or yx parameter or what is becoming more customary nowadays is to invert for some rotational invariant parameter and therefore one has not to deal with the question of rotation. There exist three such invariants, namely:

$$Z_{av} = \frac{Z_{xy} - Z_{yx}}{2}$$

$$Z_{det} = \sqrt{Z_{xx}Z_{yy} - Z_{xy}Z_{yx}}$$

$$Z_{gm} = \sqrt{-Z_{xy}Z_{yx}}$$

All these parameters give the same values for a 1-D earth response, for 2-D the *det* (determinant) and the *gm* (geometric mean) reduce to the same value but the *av* (arithmetic mean or effective) is different. For 3-D responses, all these parameters are different. A plot of these parameters in terms of apparent resistivity and phase is shown in Figure 13 for two sites. For site 080 there is a little difference between the three invariants, but the average (*ave*) is slightly different from the others which is in agreement for a 2-D case as discussed above. For site 006 in Figure 13 the *det* value is quite different than the others, showing a high degree of 3-D

It is not known which of the three invariants, if any, is best suited for 1D inversion. However several scientists have suggested that the determinant invariant is the one to use, based on the comparison of model responses for 2- and 3-D models (Park and Livelybrook, 1989; Rangabayaki, 1984; Ingham, 1988). Therefore we have chosen to use the determinant invariant impedance for the 1-D inversion.

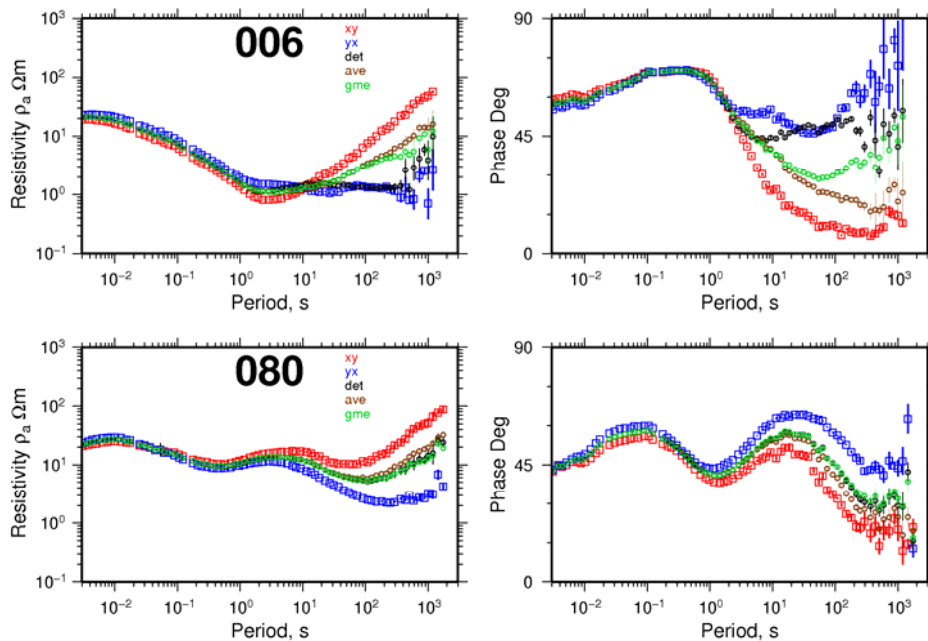


Figure 13. Apparent resistivity and phase for two sites. The different colours refer to different parameters determined from the impedance.

4.4 Telluric shift in MT soundings

The MT method, like all resistivity methods where the electric field is measured on the surface, suffers a problem called the *telluric shift* problem. The reason for this is local resistivity inhomogeneity which distorts the electric field, independent of period. The result of this is that the apparent resistivity values have an unknown multiplier (shift of logarithmic values). The TEM soundings do not suffer this problem because they measure magnetic induction in a receiver coil. By interpreting together TEM and MT soundings made at the same (or nearly the same) location, the TEM data can be used to determine the unknown multiplier of the MT apparent resistivity.

Due to this reason the TEM soundings are essential in areas where telluric shifts in MT soundings can be expected, such as in a volcanic area as in the Alid area. This is the reason for setting up the TEM site at the same, or close by the location of the MT sites. Table 1 list which TEM sounding is used for static shift correction for each MT sounding. The maximum distance between a MT site and a corresponding TEM site is 260 m (site 047).

The shift parameter is found through a joint inversion of the TEM and the MT data where the shift value for the MT apparent resistivity data is one of the inversion parameters. The inversion program used is developed at ISOR and named “temtd”. An example of an inversion results is shown in Figure 14. The MT data points are shown by blue dots (apparent resistivity and phase) and the corresponding TEM data is shown by red apparent resistivity points. The 1-D model is shown to the right and its TEM and MT response is shown by red and blue lines respectively. The model response fits the data quite well.

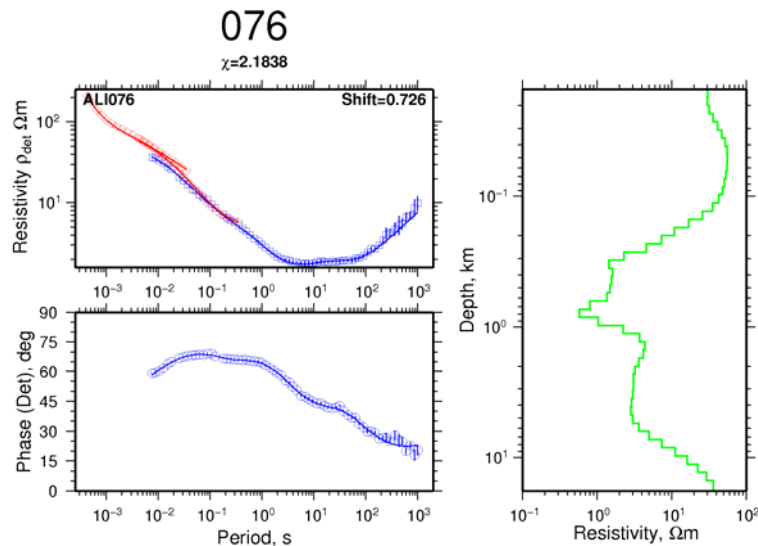


Figure 14. An example of a joint inversion result of TEM (red points) and MT data (blue points). The red and blue solid curves show the TEM and MT responses respectively of the model shown to the right. Inversion results of all the soundings are given in Appendix 5.

The distribution of all the shift parameters in the MT soundings is shown in Figure 15. If the telluric shift in the MT data is random, one would expect a mean value of 1, but as is shown in Figure 15, the mean value is about 0.7, with minimum and maximum values of 0.1 and 1.7 respectively. A shift of 0.1 means that the apparent resistivity data have been shifted down by an order of magnitude due to local resistivity inhomogeneities. Uncorrected interpretation of that sounding would have yielded a model with a resistivity about an order of magnitude lower and depths of layers about 3 times to shallow. A mean shift less than one is quite common in a volcanic environment. In Iceland similar telluric shift mean values are found as in the Alid area.

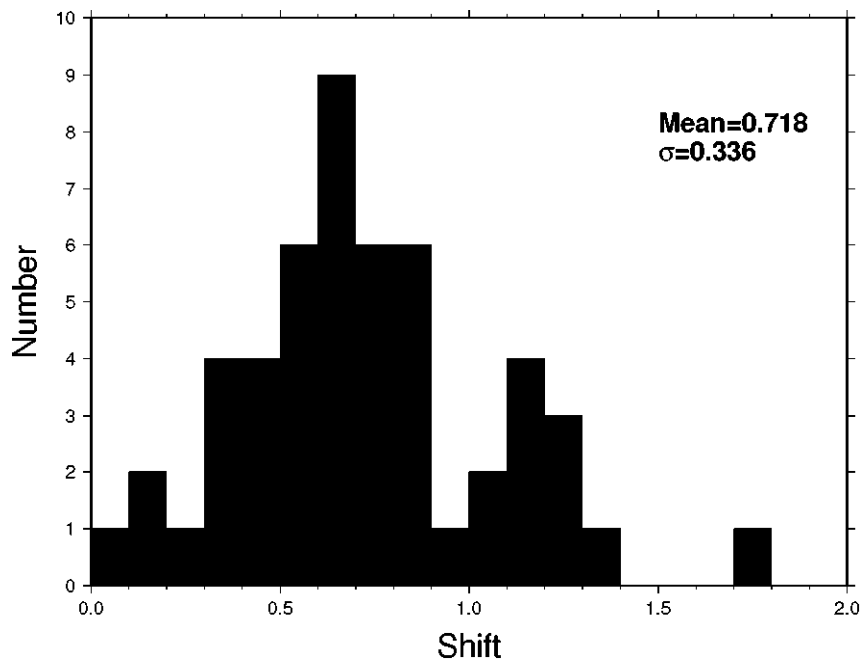


Figure 15. Histogram of shift factors applied to the MT apparent resistivity curves.

5 Result of joined inversion of MT and TEM data

The 1-D TEM/MT joint inversion results (Appendix 5) are compiled into a 3-D resistivity structure and is presented by iso-resistivity maps at different elevations above and below the sea level, and by resistivity cross sections through the survey area.

For each site a depth of exploration is estimated. At sites where only TEM sounding is present the depth of exploration is much less than the other sites, therefore those are not used at depths greater than their exploration depth which is usually not more than about 500 meters. For MT sites where data quality is bad at long periods the depth of exploration is as low as 2 km, but generally 6–10 km. In some instances where 3-D signal is strong in the long period MT data, a 1-D model could not be generated that fits both the apparent resistivity and phase, therefore the depth of penetration at those soundings is often dramatically reduces in their 1-D modelling.



Figure 16. *Fixing one of the bikes in a difficult terrain (photo: Andemariam Teklesenbet).*

5.1 Resistivity maps

Resistivity maps were drawn for resistivity at 400 and 200 metres above sea level, at sea level and 100, 200, 300, 500, 750, 1000, 1500, 2000, 2500 3000, 3500, 4000, 4500, 5000, 6000, 7000, 8000, 9000 and 10000 meters below sea level. All maps are presented in Appendix 6 but some of them will be shown and commented in the main text, in order to explain the resistivity structure of the Mt. Alid area. The elevation of the survey area is generally 100–200 metres above sea level (m a.sl.) and the soundings on top of Mt. Alid are at around 600 m a.sl. (Table 1 in Appendix 1).

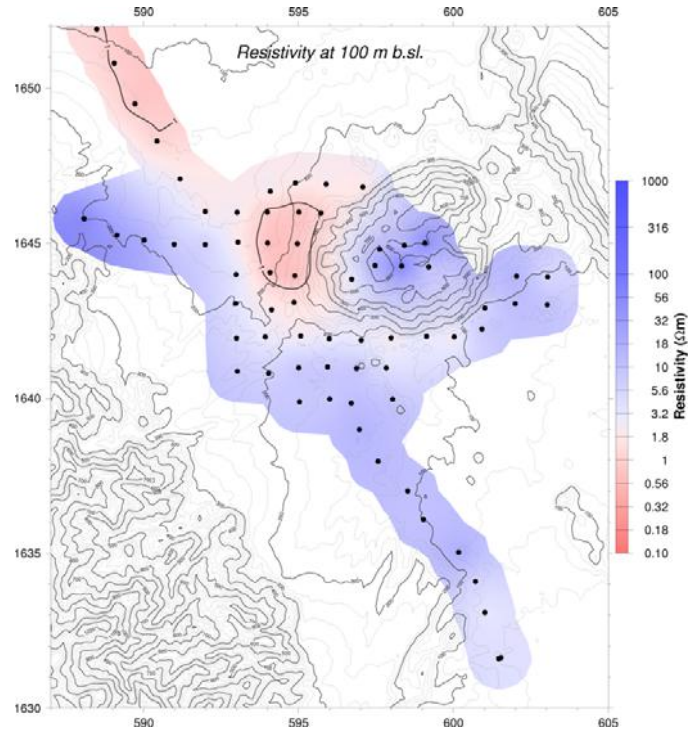


Figure 17. Resistivity map at 100 metres below sea level.

At 100 m b.sl. (Figure 17) a 1 Ωm low resistivity appears NW of Mt. Alid, which expands at deeper levels but is not observed below Mt. Alid. At 500 m.b.sl. (Figure 18) a high resistivity body appears to cut Mt. Alid in a WWS-NEE direction perpendicular to the rift system.

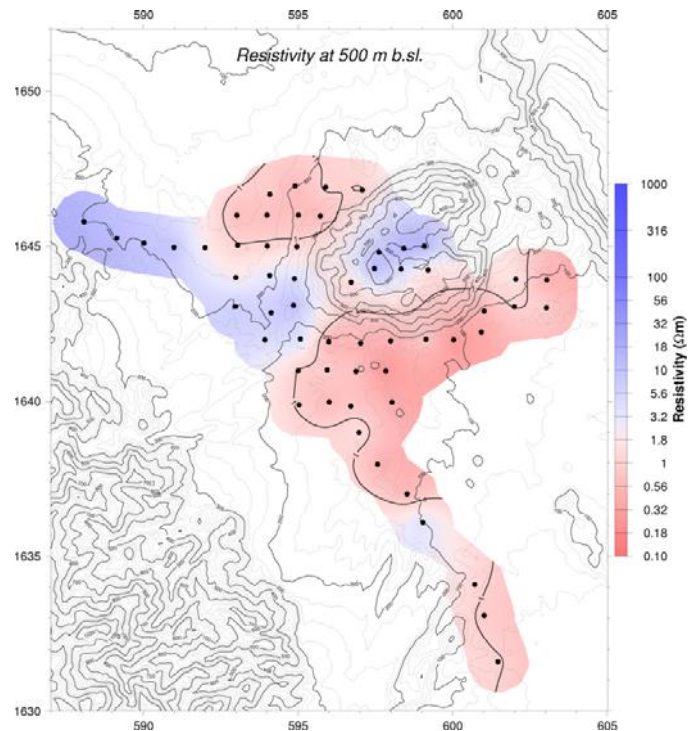


Figure 18. Resistivity map at 500 metres below sea level.

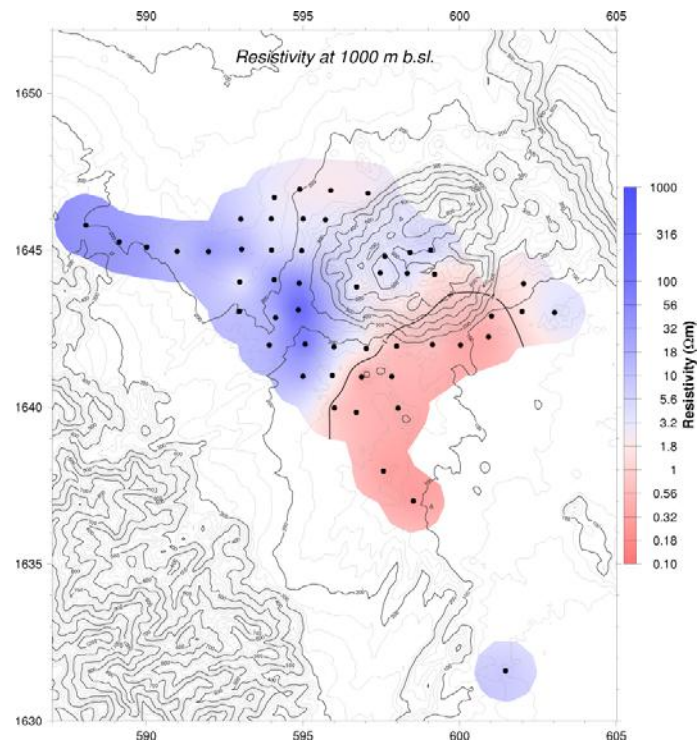


Figure 19. Resistivity map at 1000 metres below sea level.

At 1000 m.b.s.l. (Figure 19) the low resistivity west and north of Mt. Alid has disappeared and a clear SW-NE resistivity boundary is observed under the southern part of the mountain. This boundary extends down to about 2000 metres b.s.l. Below that a low resistivity appears again to the northwest of the mountain, but south and southwest of it, the low resistivity continues to deeper levels. Again no low resistivity is seen below the mountain.

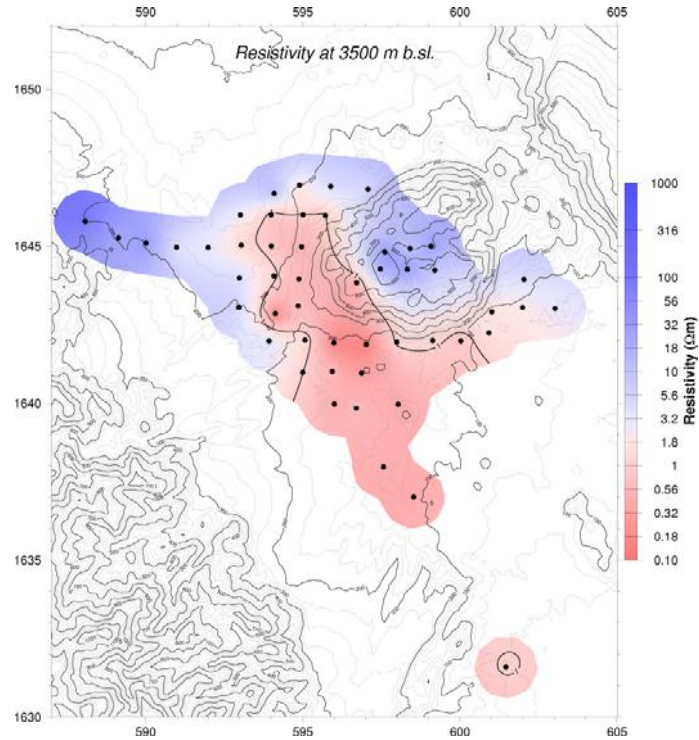


Figure 20. Resistivity map at 3500 metres below sea level.

At 3500 m.b.sl. (Figure 20) a clear low resistivity NNW-SSE body is seen west of the mountain and connected to the broader low resistivity to the south. Note that at this depth the resistivity is lowest at the base of the Mt. Alid slopes, SW of it, where the resistivity gets as low as 0.3 Ωm . There appears to be a sharp resistivity boundary in NNW-SSE direction under the western part of the mountain that extends as deep as the resolution of the soundings. This boundary is better seen in the resistivity cross sections.

Below 3500 m b.sl. the resistivity structure is similar. The low resistivity body west of the mountain widens, and a clear low resistivity region is observed at the base of the mountain southwest of it (see Figures in Appendix 6).

5.2 Resistivity cross sections

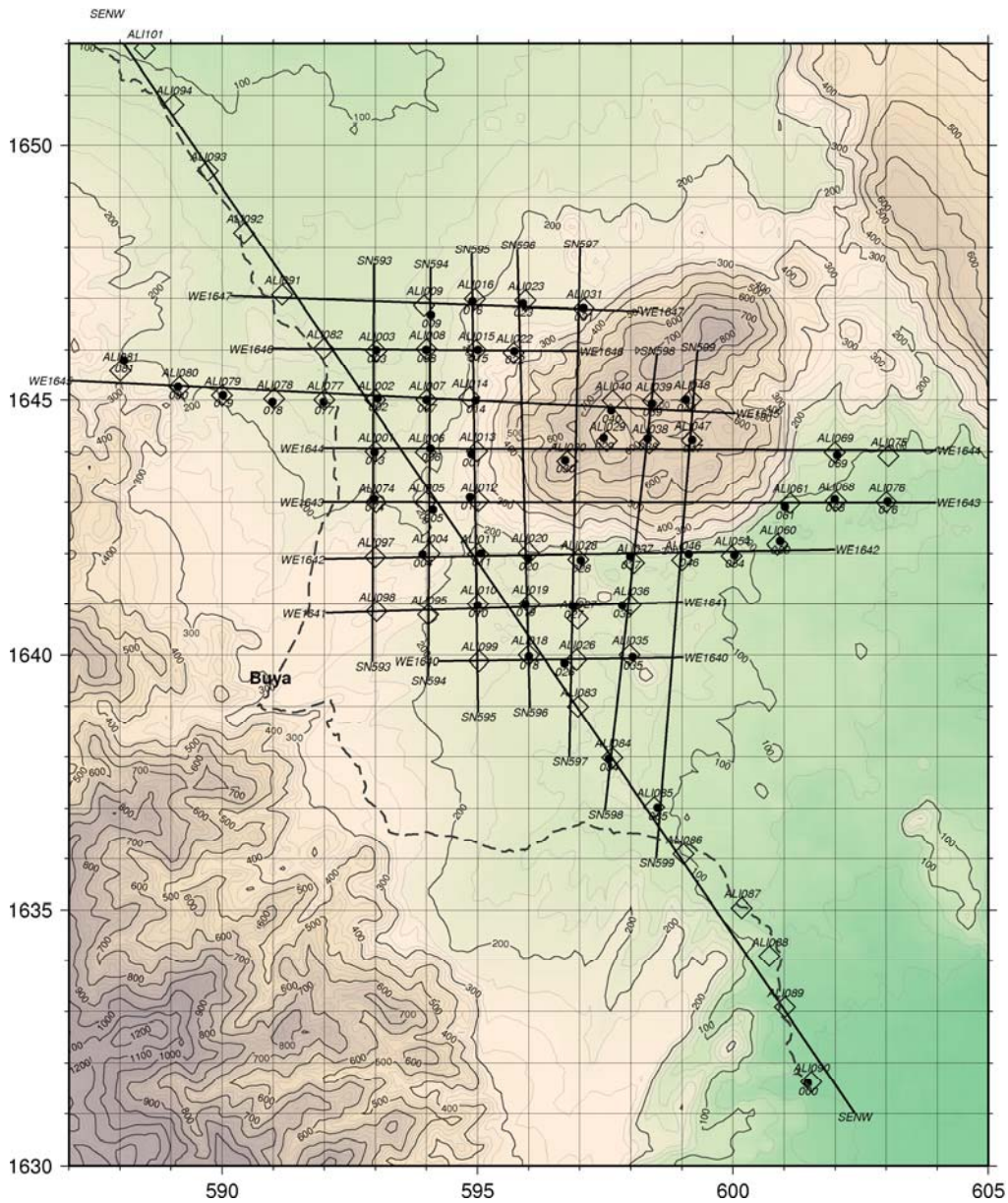


Figure 21. Location of cross sections.

Figure 21 shows the location of the cross sections shown on Figures 22 through 37. On all the figures no resistivity is shown below the estimated depth of resolution for each sounding. The name of the WE and SN sections are derived from the north and east UTM coordinates.

One 25 km long SE-NW resistivity cross section is presented, as well as 8 cross sections bearing west-east direction and 7 cross sections bearing north-south direction.

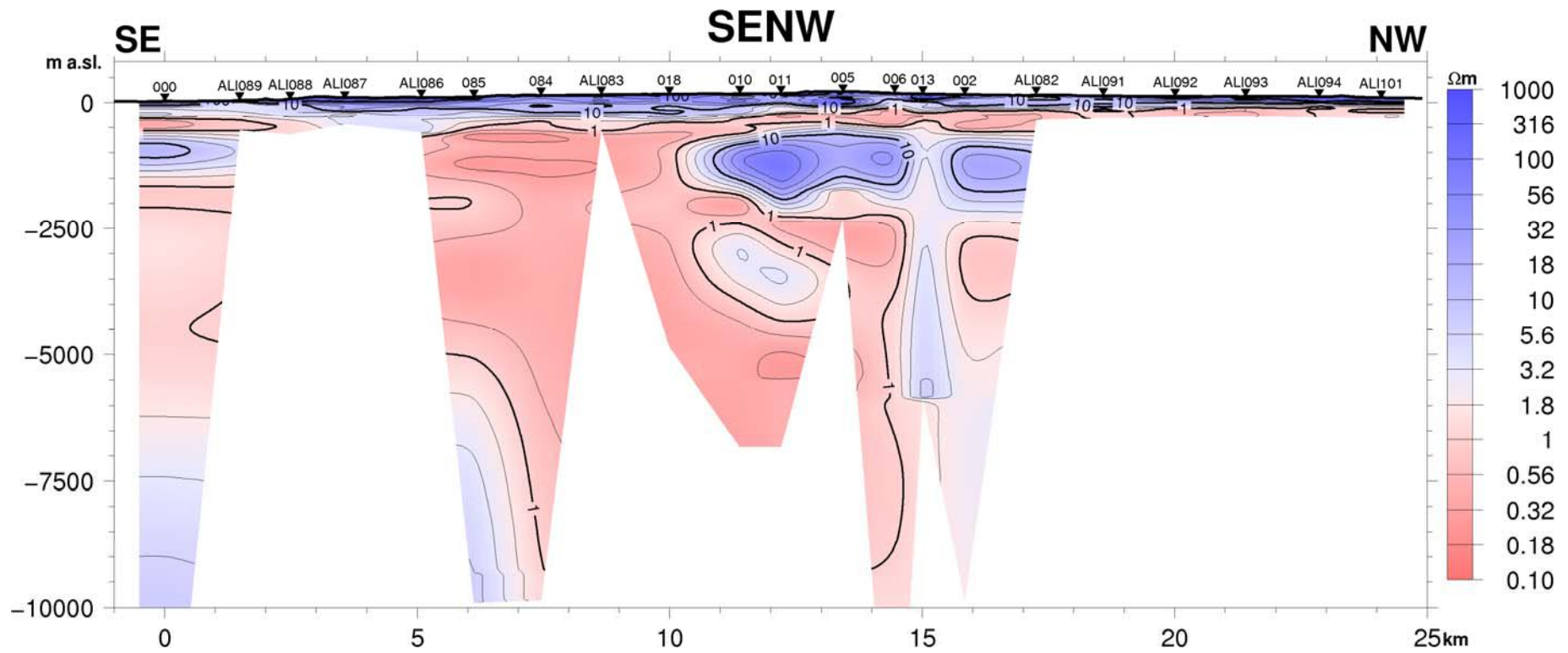


Figure 22. A resistivity cross section through the area, with NW-SE direction.

The long SE-NW resistivity cross section is shown on Figure 22. Its location is west of Mt. Alid (see Fig. 20). The southernmost site is the base station. All soundings with the name starting with ALI show the result from the TEM measurements only and therefore they have a shallow depth penetration. There was not enough time also to measure MT soundings at those locations. The data clearly show a conductive shallow layer through the whole area at a few hundred metres depth. The sharp vertical resistivity boundary between sites 018 and 010, at the depth of 1–2 km b.sl. is very clear. South of this boundary the shallow low resistive layer adjoins to the deeper low resistivity body, seen at 1.5–2.5. km b.sl.. The fact that this deeper low resistivity body is seen in the southern most sounding (000), approximately 10 km away from the mountain, suggests that it exist over a very large area. However, its conductivity is somewhat lower there, than in the vicinity of Mt. Alid.

The next 8 cross sections have a west-east direction and they are shown on Figures 23 through 30. The southernmost cross section (Figure 23) shows clearly the extent of the large low resistivity body to the south and south west of the mountain. Sections WE1641 and WE1642 , (Figures 24 and 25) show that the low resistivity area is bounded to the west. Section WE1643 (Figure 26) has no soundings in the middle and therefore resistivity values are not shown at depth there. This sections shows two low resistivity layers, one at shallow depth (~200 m. b. sl.) and another at 2–3.5 km b. sl. It is clear that this section is located in a highly 3-D environment and therefore the deeper part is badly resolved with the 1-D interpretation technique used here. Sections WE1644 and WE1645 (Figures 27 and 28) clearly show the low resistivity body west of Mt. Alid. There appears to be a very sharp vertical boundary running NS under the western part of the mountain. The next two sections, WE1646 and WE1647 (Figures 29 and 30), show that the low resistivity body is not as clear to the north, and is clearly bounded in the west.

The SN oriented sections are shown on Figures 31 trough 37. Some of those sections are very short. All these sections show the vertical EW oriented resistivity boundary which runs through the southern part of Mt. Alid. Sections SN594, SN595 and SN596 (Figures 32–34), show that the NS oriented low resistivity body west of the mountain is not seen at the northernmost sites.

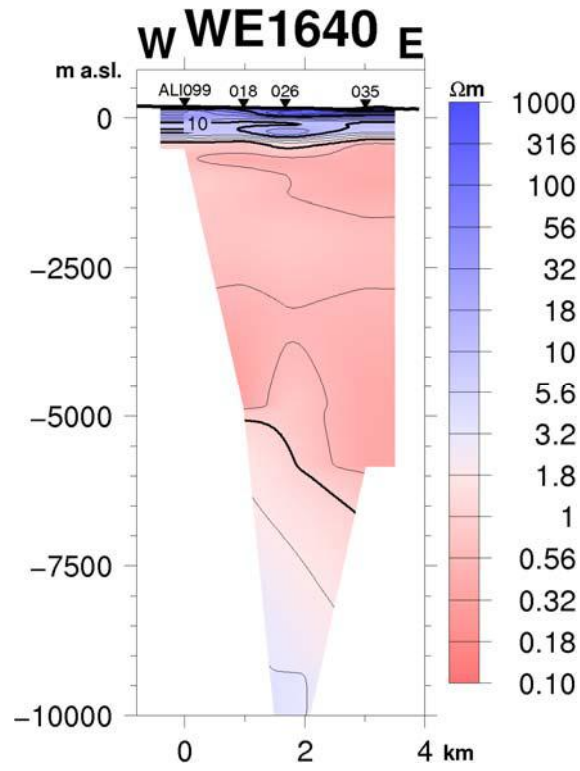


Figure 23. Cross section WE1640.

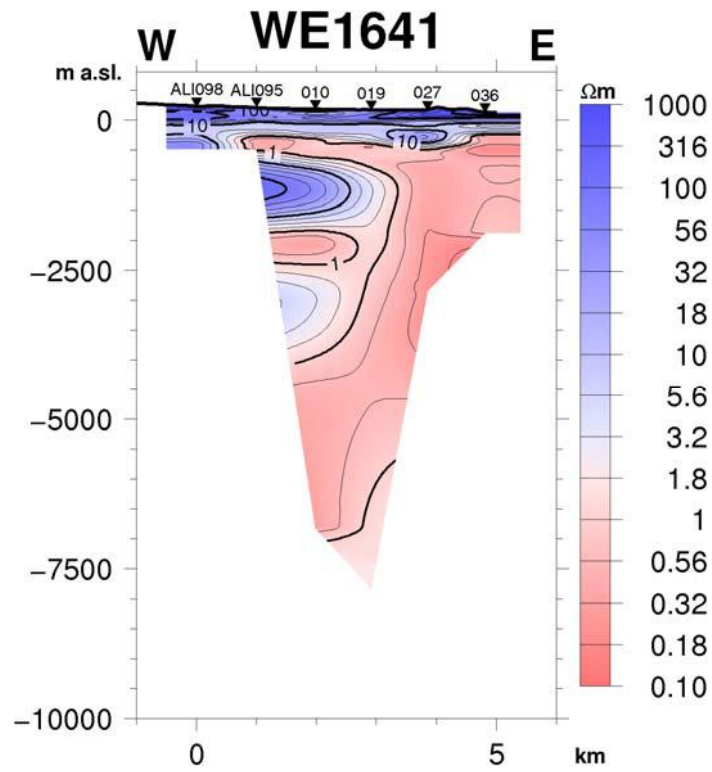


Figure 24. Cross section WE1641.

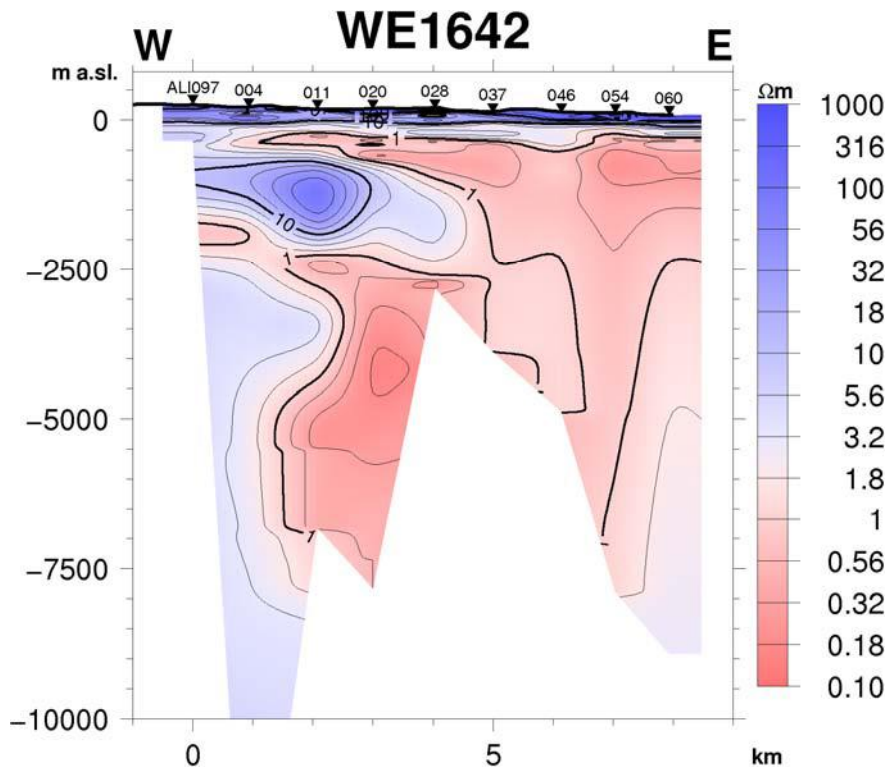


Figure 25. Cross section WE1642.

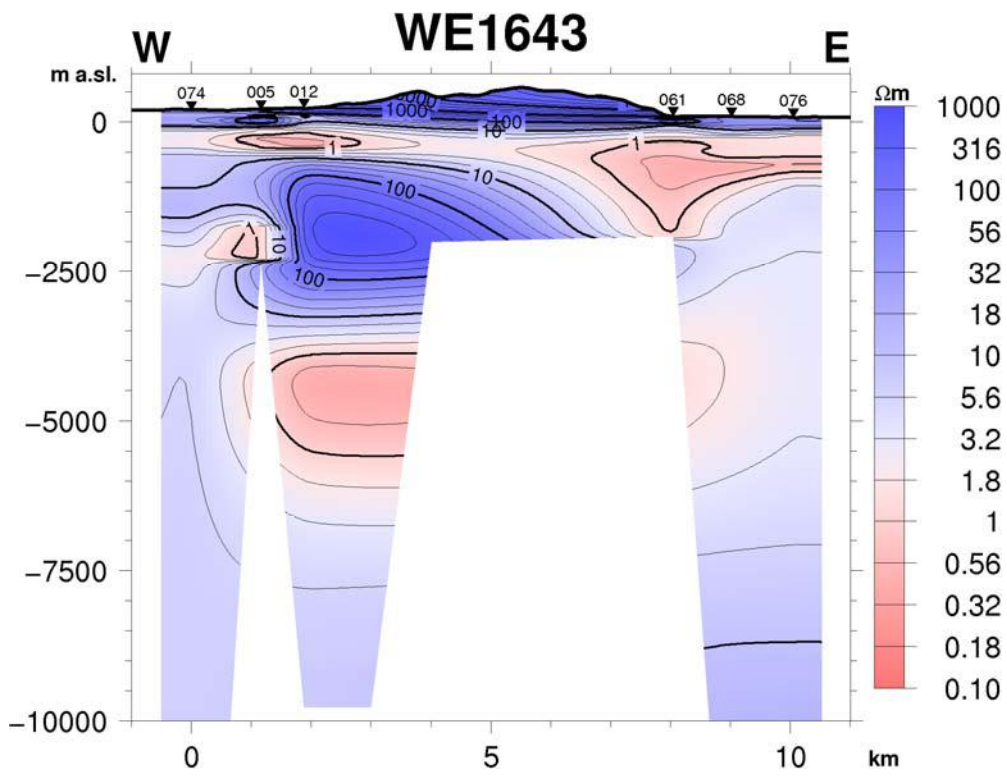


Figure 26. Cross section WE1643.

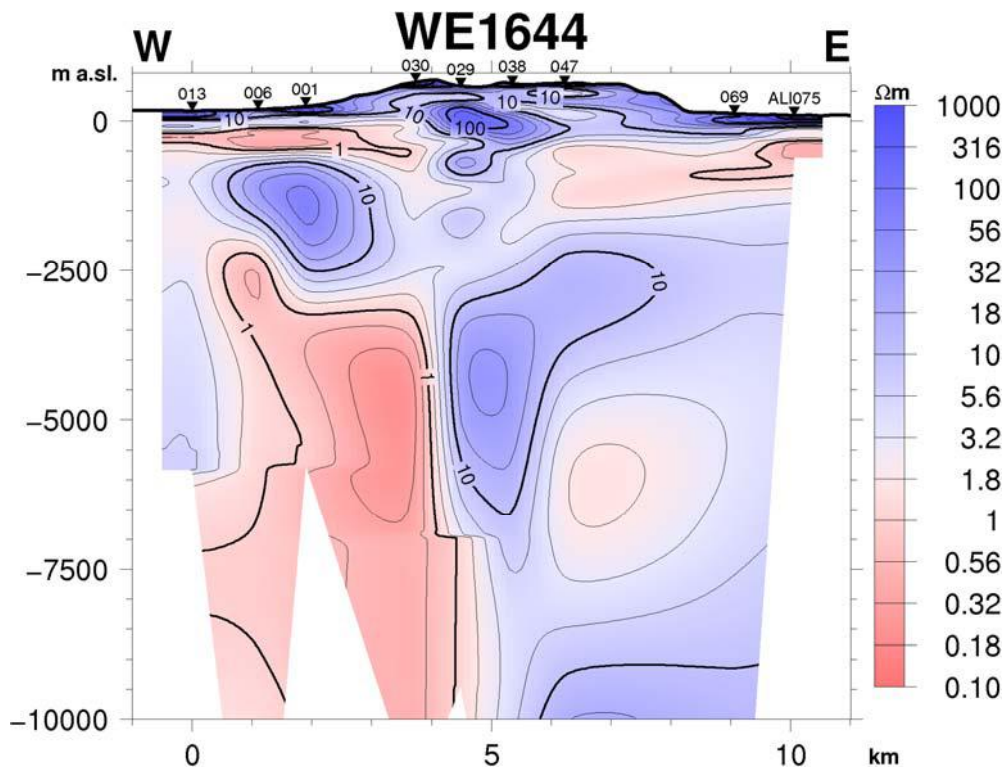


Figure 27. Cross section WE1644.

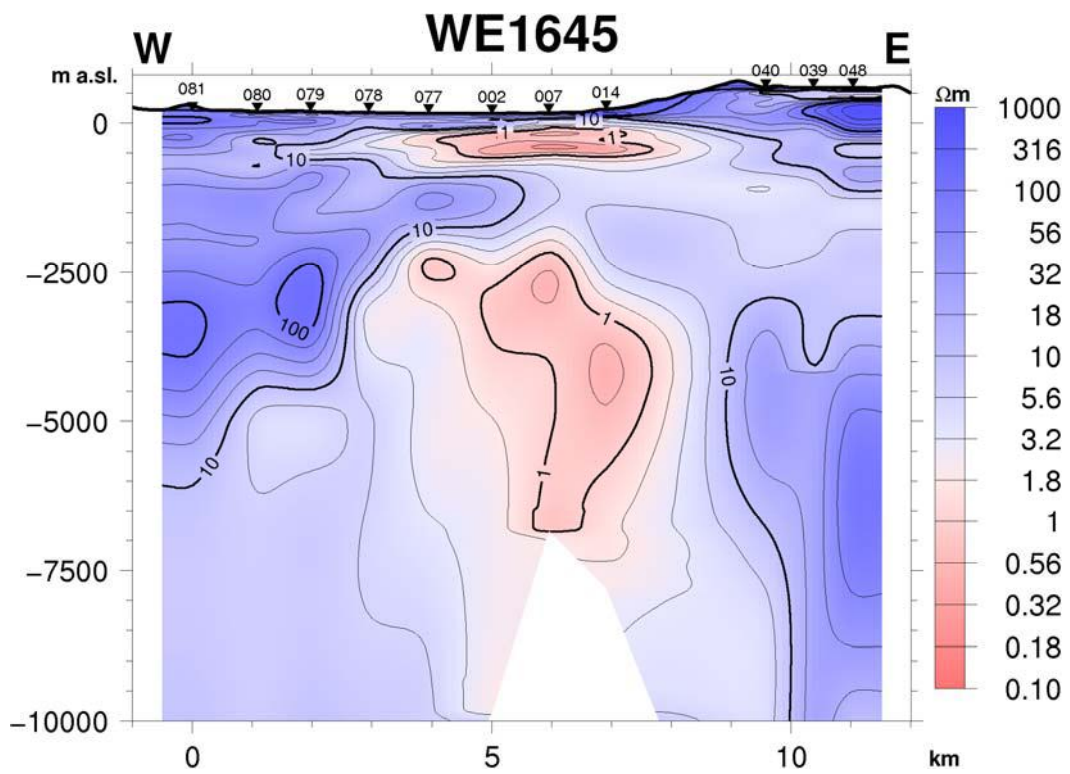


Figure 28. Cross section WE1645.

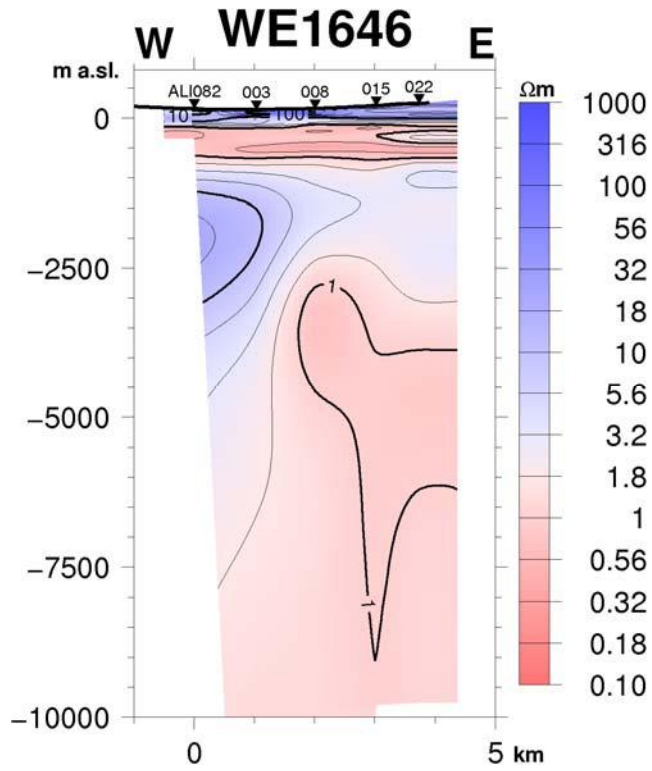


Figure 29. Cross section WE1646.

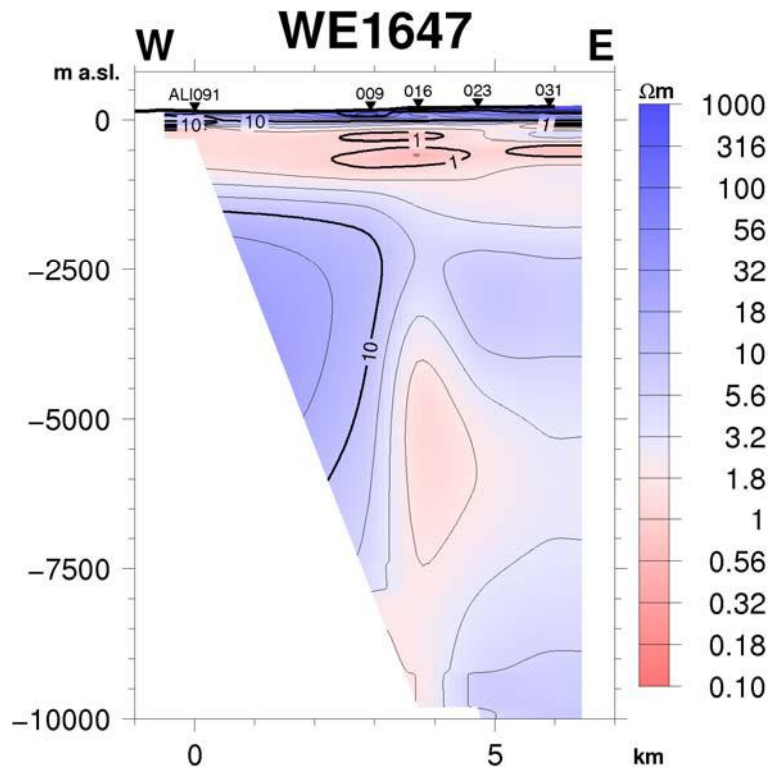


Figure 30. Cross section WE1647.

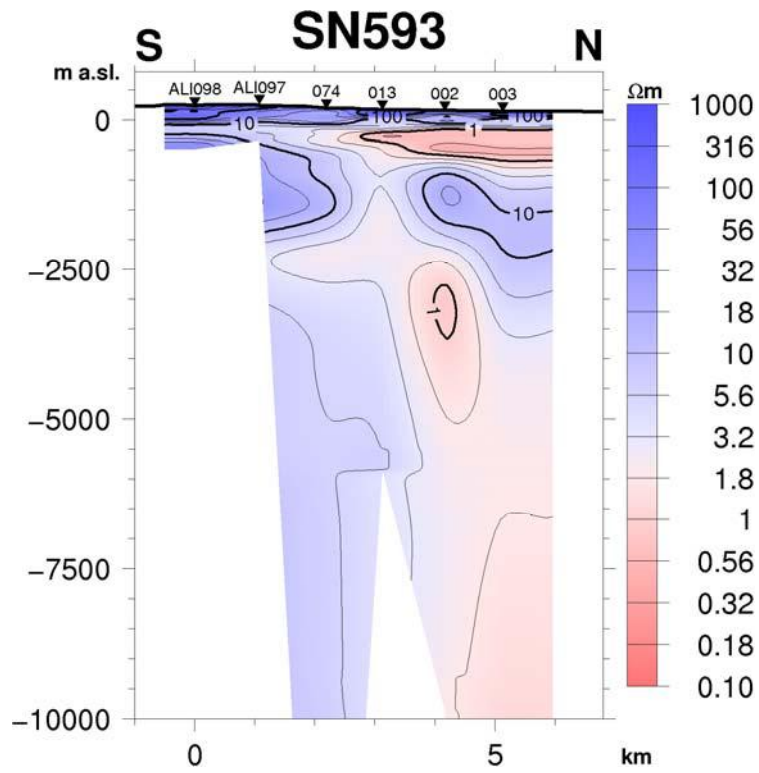


Figure 31. Cross section SN593.

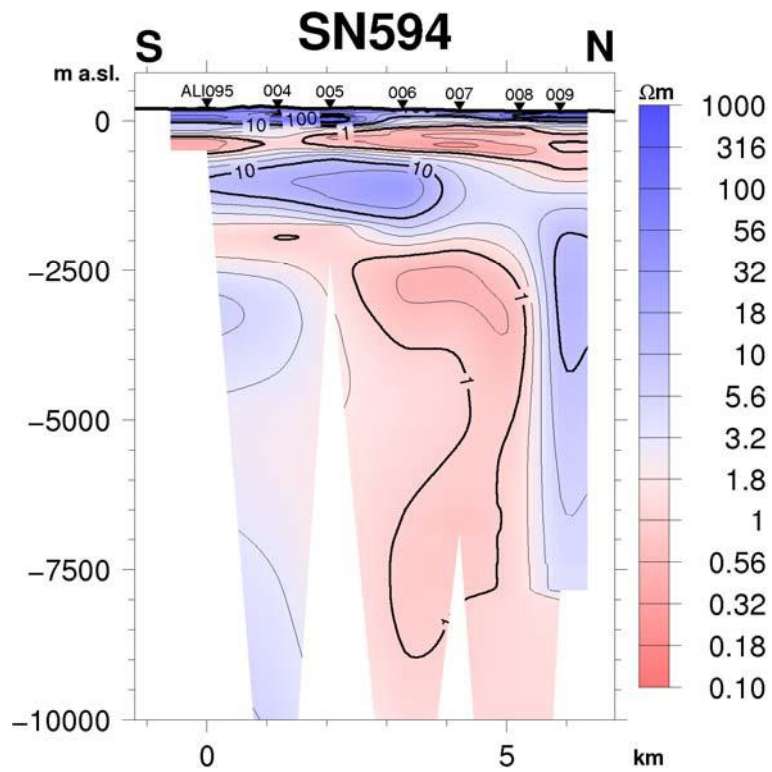


Figure 32. Cross section SN594.

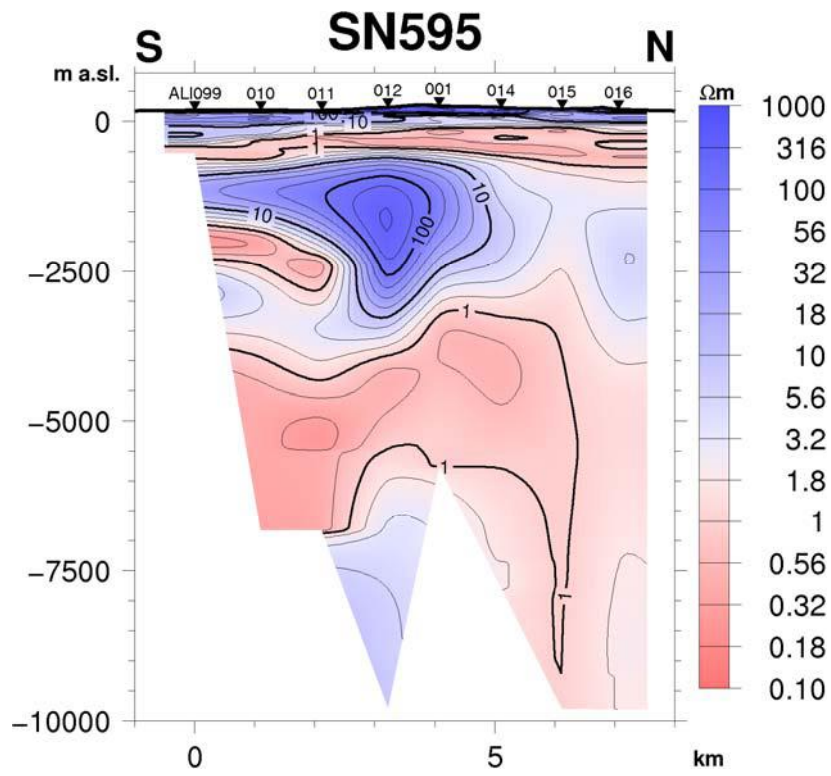


Figure 33. Cross section SN595.

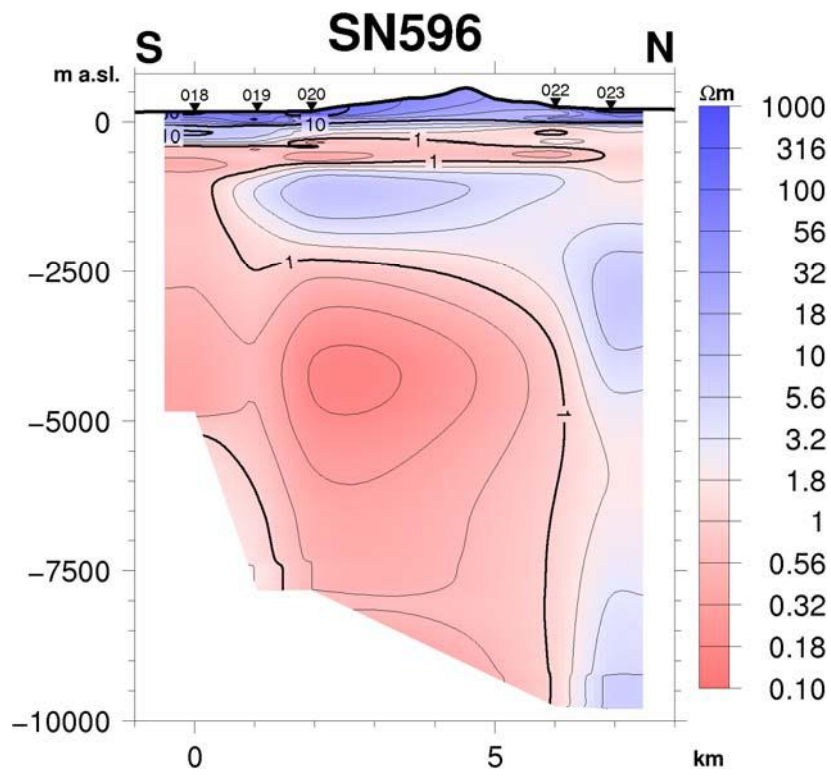


Figure 34. Cross section SN596.

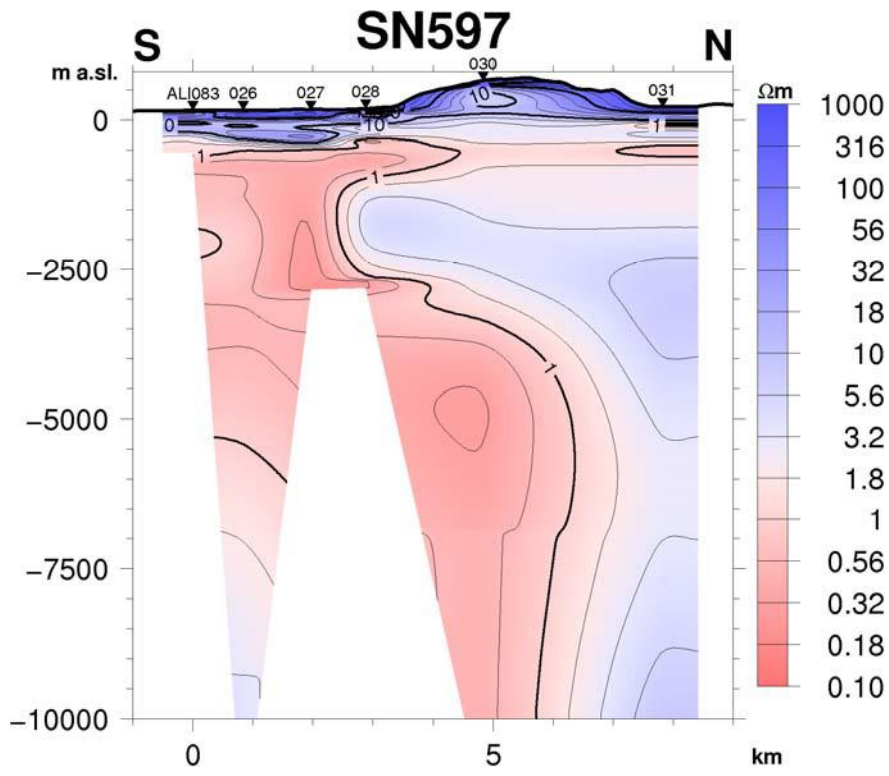


Figure 35. Cross section SN597.

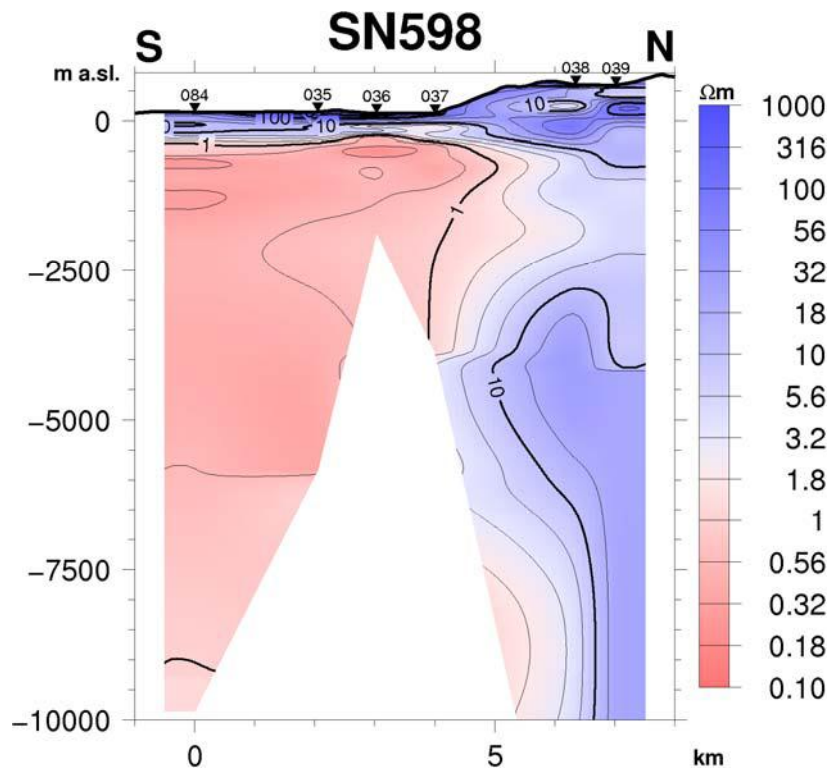


Figure 36. Cross section SN598.

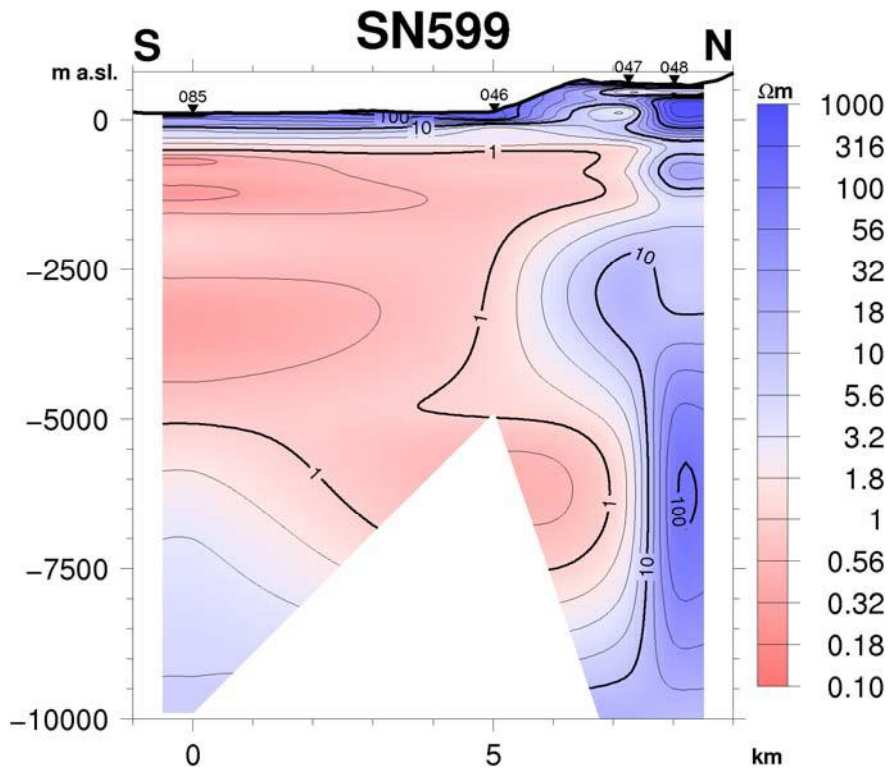


Figure 37. Cross section SN599.

6 Conclusions and recommendations

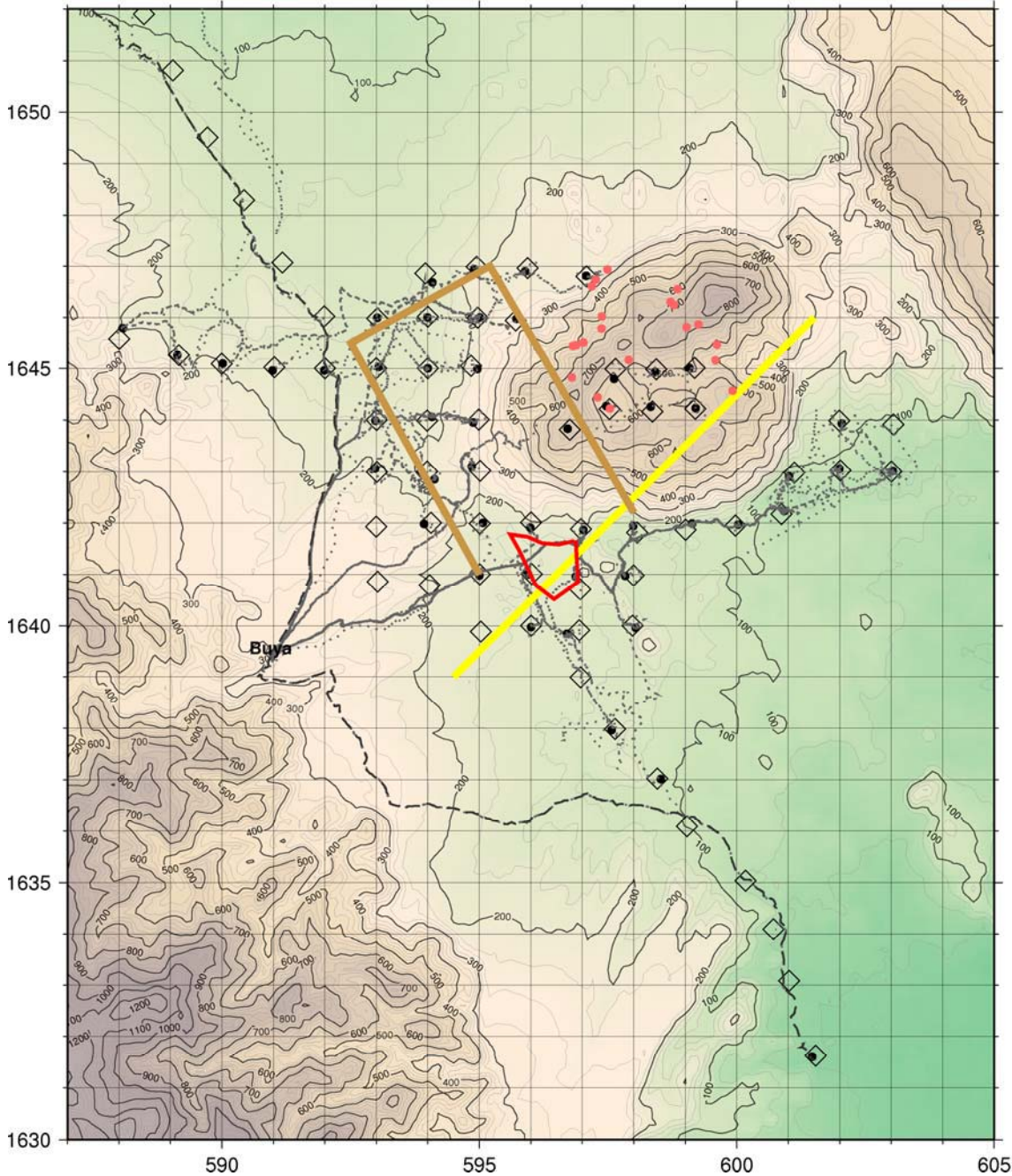


Figure 38. The Yellow line shows the location of the vertical resistivity boundary between 1/2 and 2 km depth. The brown contour lines outline the low resistivity body west of Mt. Alid at about 2 km depth. Red dots are geothermal vents on Mt. Alid (data from Geological survey of Eritrea), and the red polygon is the area of enhanced vegetation discussed in the text.

The resistivity structures of the Alid area are characterized by the following main features:

- **A thin low resistivity layer.** A shallow (at a few hundred metres depth) and thin (few hundred metres) low resistivity layer is seen in most of the soundings, except in those soundings on the top of Mt. Alid.
- **A SW-NE Lineament.** A conductive zone is seen down to about 6–7 km depth (and even more in some places) in the south and southwest of Mt. Alid. This zone has a sharp vertical boundary or a lineament in the depth interval from ½–2 km depth shown by a yellow line on Figure 38. This boundary is best seen on the iso-resistivity map at 1 km b.sl. on Figure 19.
- **A low resistivity body.** Below the western part of Mt Alid and to the west of the mountain there is a low resistivity body, approximately 3 km wide and with a NNW-SSE direction. It reaches the highest elevation at 2–3 km b.sl., and extending down to a depth of about 7 km. The location of this body is shown on Figure 38, marked with a brown contour line.
- Beneath most of Mt Alid there is a rather **high resistivity**, compared to the surroundings, and no deep conductor, except in the westernmost sounding on the mountain.



Figure 39. *An oases in the middle of the dry volcanic landscape. Most likely the cause of geothermal activity below the surface (photo: Hjálmar Eysteinnsson).*

How can these resistivity structures relate to the geothermal system?

The thin low resistivity layer seen down to 1000 metres depth is interpreted as the old conductive sea bed.

According to Lowenstern et al. (1999), geological and geochemical studies imply that a high temperature geothermal system underlies the Alid volcanic center. The resistivity survey does not cover enough area to compare the resistivity structure beneath Mt. Alid to the structures surrounding it. The high resistivity beneath Mt. Alid does not stand out as an anomaly, as it is not bounded to the east and north-east in lack of soundings. Until we see, if the high resistivity represents a resistive body in low resistivity surroundings we can't conclude that this high resistivity represents the geothermal heat source.

If this, however, were the case, i.e. the high resistivity under Mt. Alid represented the heat source, one would expect it to be imbedded in low resistivity surroundings. From the results of this survey we see that the high resistivity has a very sharp SW-NE boundary with the low resistivity on the southern side. This boundary forms a clear lineament extending from the depth 500m .b.sl. down to 2000m b.sl. From the depth of 3500 down as far as can be detected there is a distinctive low resistivity body south-west of Mt. Alid. These low resistivity bodies to the south and west of the mountain could well be the part of a greater area surrounding Mt. Alid, but as of now, we do not have information on the resistivity to the east and northeast.

The lineament mentioned is sure to play a major role in the geothermal system. It most likely represents a SW-NE fault or a fault system that cuts under the southern part of the mountain. According to Clynne et al. (2005), some fumaroles on the top of the mountain, form weak N45°E alignments, the same direction as the lineament. The major axis of the mountain itself has this direction. A geological map, in the paper of Clynne et al., shows a shift in the fissure swarm through Mt Alid, where it intersects the NE-SW lineament. This could possibly indicate that the SW-NE lineament represents a transform fault underlying Mt. Alid.

At the SW slopes of Mt. Alid, an area, the size of about 1 km², shows quite a different character in vegetation than the surrounding dry volcanic landscape (see Figure 38). The growth of the vegetation is clearly influenced by water or moisture in the ground. It is reasonable to expect that this is due to steam, coming from the geothermal system below. This area is shown on Figure 38, marked by a red polygon. The area coincides with the NE-SW lineament, marked as a yellow line on the figure. This supports the idea that the transform fault or connected fault system takes part in, or controls the upflow into the geothermal system.

With the information available on the resistivity structures, it is more difficult to explain the deep seated low resistivity body below the western part and west of Mt. Alid (brown contour lines on Figure 38). It is reasonable to assume that resistivity at such depths is influenced by high temperatures. It is also interesting to observe that the vegetated area is right above the top of the low resistivity body. However, this distinctive low resistivity body has to be seen in a greater context to be better understood. The main features are marked on an aerial photo of the study area from Google-Earth (<http://earth.google.com>) in figure 40.

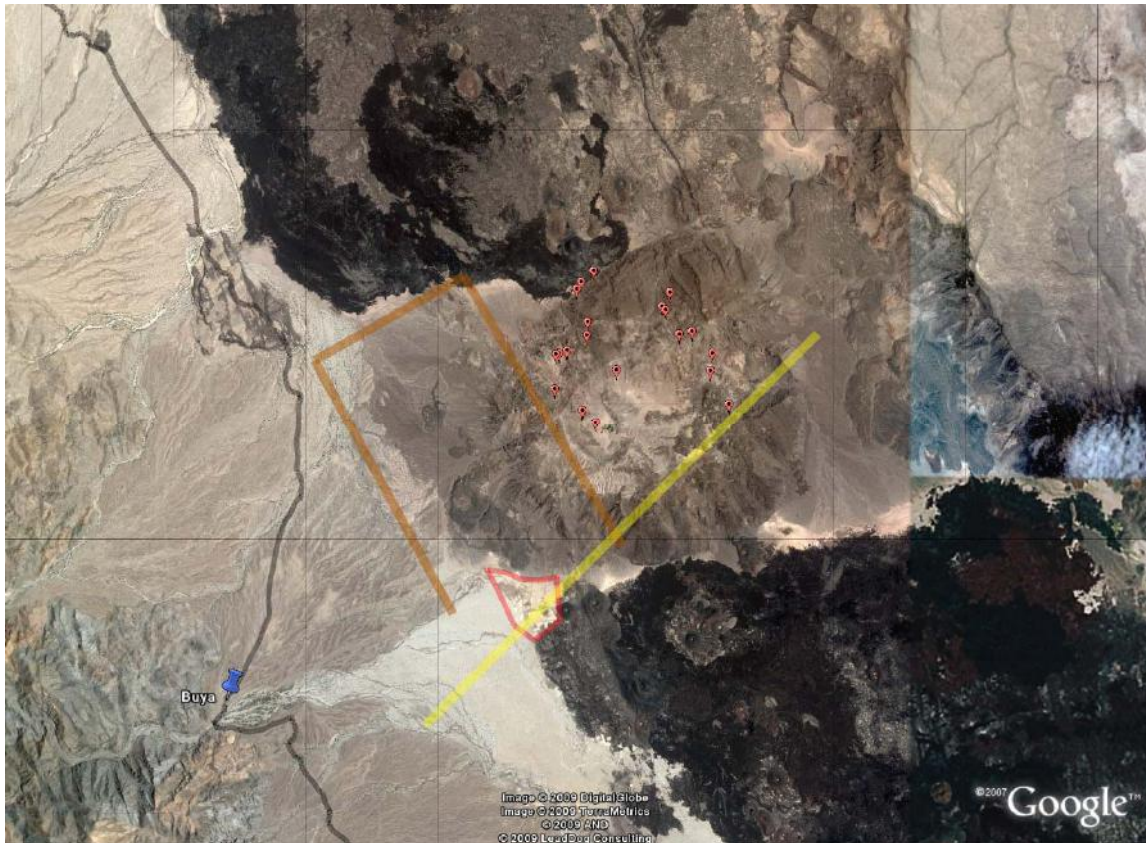


Figure 40. An aerial photo of Mt. Alid and part of the Danakil depression from Google-earth. The main features from the resistivity survey are shown as: a yellow line (the transform fault) and the brown contour lines (the deep seated low-resistivity body). The red polygon outlines the vegetated area and red dots show geothermal manifestations.

Recommendations of further studies:

While surveying the area, the geophysicists came across steam vents/springs not present on any maps. Some of them were found by the direction of the local people.

- A careful mapping of all geothermal surface manifestations is recommended with directions from the local people. This could give invaluable information on the geothermal activity in the area and the size of the geothermal field.

The original survey plan covered Mt. Alid and nearest vicinity. It was however not possible to survey the area to the northeast and north of the mountain within the given timeframe. The terrain also turned out to be difficult, at times inaccessible but some parts of the lava could possibly be accessed with the aid of camels for the transportation of the equipment.

- It is recommended to explore if further resistivity surveying is possible to the NE of the present survey area. It is also recommended to finish the MT survey in the long NW-SE profile where only TEM soundings are present.

Quite much of the MT data in this study shows a high degree of three-dimensionality. Therefore a 3-D modeling of the area is called for to fully explain the data. Such modeling might well change the resistivity picture given in this report, how much is impossible to say until the modeling has been done.

- It is recommended that the data should be interpreted with a 3-D modeling program.

A resistivity profile across the rift depression, further away from the Alid area would give valuable information on the resistivity differences between areas far away from geothermal activity and close to it, i.e. what resistivity structure is normal and what caused by geothermal activity.

- It is recommended to extend the soundings to a profile across Danakil depression

As tectonics play the major role in geothermal activity it is valuable to see if tectonic movements take place in the Mt. Alid area, and map the seismically active structures.

- A seismicity survey is recommended.

A gravity Bouguer map would be a valuable tool to evaluate density difference in the upper part of the crust. Intrusive bodies are likely to be heat source for the geothermal system and could be identified with gravity mapping.

- A gravity survey is recommended, especially if a full resistivity survey turns out to be impossible

Iceland GeoSurvey would like to extend its gratitude to the Geological Survey of Eritrea for their cooperation in this project. This was a hard work, often challenging due to the difficult terrain and the short time frame. Without their cooperation this project would not have been possible to implement.

7 References

- Barberi F. and Varet Jacques (1977). *Volcanism of Afar: Small-scale plate tectonic implications*. Geological Society of America Bulletin. v 88. p 1251-1266.
- Clynne, M. A., Duffield, W. A., Fournier, R. O., Woldegiorgis, L., Janik, C. J., Kahsai, G., Lowenstern, J. B., Weldemariam, K., Smith, J. G. and Tesfai, T. (2005). *Proceedings World Geothermal Congress 2005, Antalya, Turkey*. 24.–29. April 2005.
- Ingham, M. R. (1988). The use of invariant impedances in magnetotelluric interpretation. *Geophysical Journal*, 92, 165–169.
- Lowenstern, J. B., Janik, C. J., Fournier, R. O., Tesfai, T., Duffield, W. A., Clynne, M. A., Smith, J. G., Woldegiorgis, L., Weldemariam, K. and Kahsai, G. (1999). *A geochemical reconnaissance of the Alid volcanic center and the geothermal system, Danakil depression, Eritrea*. *Geothermics*. p 161–187.
- Park, S. K. and Livelybrook, D. W. (1989). Quantitative interpretation of rotationally invariant parameters in magnetotellurics. *Geophysics*, 54, 1483–1490.
- Rangabayaki, R. P. (1984). An interpretive analyses of magnetotelluric data. *Geophysics* 49, 1730–1748.
- Sternberg, B. K., Washburne, J. C. and Pellerin, L. (1988). Correction for the static shift in magnetotelluric, using transient electromagnetic soundings. *Geophysics*, 53, 1459–1468.

